# Inhibition of oxytocin and vasopressin neuron activity in rat hypothalamic paraventricular nucleus by relaxin-3–RXFP3 signalling

Alan Kania[1], Anna Gugula[1], Agnieszka Grabowiecka[1], Camila de Ávila[2], Tomasz Blasiak[1], Zenon Rajfur[3], Marian H. Lewandowski[1], Grzegorz Hess[1,4], Elena Timofeeva[2], Andrew L. Gundlach[5,6,7] iD and Anna Blasiak[1] iD

[1]*Department of Neurophysiology and Chronobiology, Institute of Zoology, Jagiellonian University, 30-387 Krakow, Poland*

[2]*Faculté de Médecine, Département de Psychiatrie et de Neurosciences, Centre de Recherche de l'Institut Universitaire de Cardiologie et de Pneumologie de Québec, Université Laval, Québec, QC, Canada G1V 0A6*

[3]*Faculty of Physics, Astronomy and Applied Computer Science, Institute of Physics, Jagiellonian University, 30-348 Krakow, Poland*

[4]*Institute of Pharmacology, Polish Academy of Sciences, 31-343 Krakow, Poland*

[5]*The Florey Institute of Neuroscience and Mental Health, Parkville, VIC 3052, Australia*

[6]*Florey Department of Neuroscience and Mental Health, The University of Melbourne, VIC 3010, Australia*

[7]*Department of Anatomy and Neuroscience, The University of Melbourne, VIC 3010, Australia*

*The Journal of Physiology*

## Key points

- Relaxin-3 is a stress-responsive neuropeptide that acts at its cognate receptor, RXFP3, to alter behaviours including feeding. In this study, we have demonstrated a direct, RXFP3-dependent, inhibitory action of relaxin-3 on oxytocin and vasopressin paraventricular nucleus (PVN) neuron electrical activity, a putative cellular mechanism of orexigenic actions of relaxin-3.
- We observed a $G\alpha_{i/o}$-protein-dependent inhibitory influence of selective RXFP3 activation on PVN neuronal activity *in vitro* and demonstrated a direct action of RXFP3 activation on oxytocin and vasopressin PVN neurons, confirmed by their abundant expression of *RXFP3* mRNA. Moreover, we demonstrated that RXFP3 activation induces a cadmium-sensitive outward current, which indicates the involvement of a characteristic magnocellular neuron outward potassium current.
- Furthermore, we identified an abundance of relaxin-3-immunoreactive axons/fibres originating from the nucleus incertus in close proximity to the PVN, but associated with sparse relaxin-3-containing fibres/terminals within the PVN.

**Abstract** The paraventricular nucleus of the hypothalamus (PVN) plays an essential role in the control of food intake and energy expenditure by integrating multiple neural and humoral inputs. Recent studies have demonstrated that intracerebroventricular and intra-PVN injections of the neuropeptide relaxin-3 or selective relaxin-3 receptor (RXFP3) agonists produce robust feeding in satiated rats, but the cellular and molecular mechanisms of action associated with these orexigenic effects have not been identified. In the present studies, using rat brain slices, we demonstrated that relaxin-3, acting through its cognate G-protein-coupled receptor, RXFP3, hyperpolarized a majority of putative magnocellular PVN neurons (88%, 22/25), including cells producing the anorexigenic neuropeptides, oxytocin and vasopressin. Importantly, the action of relaxin-3 persisted in the presence of tetrodotoxin and glutamate/GABA receptor antagonists, indicating its direct action on PVN neurons. Similar inhibitory effects on PVN oxytocin and vasopressin

A. Gugula and A. Grabowiecka contributed equally to this work.

neurons were produced by the RXFP3 agonist, RXFP3-A2 (82%, 80/98 cells). *In situ* hybridization histochemistry revealed a strong colocalization of *RXFP3* mRNA with oxytocin and vasopressin immunoreactivity in rat PVN neurons. A smaller percentage of putative parvocellular PVN neurons was sensitive to RXFP3-A2 (40%, 16/40 cells). These data, along with a demonstration of abundant peri-PVN and sparse intra-PVN relaxin-3-immunoreactive nerve fibres, originating from the nucleus incertus, the major source of relaxin-3 neurons, identify a strong inhibitory influence of relaxin-3–RXFP3 signalling on the electrical activity of PVN oxytocin and vasopressin neurons, consistent with the orexigenic effect of RXFP3 activation observed *in vivo*.

**Corresponding authors** Anna Blasiak: Department of Neurophysiology and Chronobiology, Jagiellonian University, Gronostajowa 9, 30-387 Krakow, Poland.    Email: anna.blasiak@uj.edu.pl
Andrew L. Gundlach: The Florey Institute of Neuroscience and Mental Health, 30 Royal Parade, Parkville, VIC 3052, Australia.    Email: andrewlg@unimelb.edu.au

**Abbreviations**    ACSF, artificial cerebrospinal fluid; ACTH, adrenocorticotrophic hormone; AP-5, 2-amino-5-phosphopentanoic acid; AVP, arginine vasopressin; CNQX, 6-cyano-7-nitroquinoxaline-2,3-dione; CRH, corticotrophin-releasing hormone; Ir, immunoreactive/immunoreactivity; KPBS, potassium phosphate-buffered saline; NI, nucleus incertus; OT, oxytocin; PKC, protein kinase C; PVN, paraventricular nucleus of the hypothalamus; RXFP, relaxin family peptide receptor; RXFP3-A2, RXFP3-selective relaxin-3 analogue 2 ([R3A(11-24,C15→A)B]).

# Introduction

The paraventricular nucleus of the hypothalamus (PVN) is often considered as the main autonomic brain centre, and a large range of neurotransmitters and neuropeptides synthesized in different classes of PVN neurons control energy homeostasis and body fluid balance [e.g. oxytocin (OT) and arginine vasopressin (AVP)], reproduction (dopamine and OT), growth and development (somatostatin) and the hypothalamic–pituitary–adrenal and hypothalamic–pituitary–thyroid axes [corticotrophin-releasing hormone (CRH) and thyrotrophin-releasing hormone, respectively; Ferguson *et al.* 2008)]. In turn, many modulatory extrinsic inputs to the PVN tightly regulate its activity, often via G-protein-coupled receptor signalling (Hazell *et al.* 2012). Whole-cell patch-clamp recordings of PVN neuron activity combined with immunohistochemical profiles have identified a useful grouping of PVN cells into the following three different types: (i) magnocellular neurosecretory neurons that secrete OT and AVP into the posterior pituitary gland (electrophysiological type I); (ii) parvocellular neurosecretory neurons that secrete hypophysiotrophic hormones; and (iii) parvocellular pre-autonomic neurons innervating spinal autonomic centres (2 and 3, which are electrophysiological type II; Lee *et al.* 2012).

Oxytocin and AVP are hormones that strongly influence feeding behaviour. It has been shown in both animals and humans that OT acts as an anorexigenic signal (Sabatier *et al.* 2013; Kim *et al.* 2015; Klockars *et al.* 2015), and deficiencies in OT synthesis lead to hyperphagia and obesity (Kublaoui *et al.* 2008). Likewise, AVP is considered to be an anorexigenic factor (Aoyagi *et al.* 2009), and intracerebroventricular or intraperitoneal injections of OT and AVP lead to reductions in food intake (Meyer

*et al.* 1989; Arletti *et al.* 1990; Morton *et al.* 2012). Release of OT from dendrites of magnocellular PVN neurons is also thought to allow for oxytocinergic control of distant hypothalamic nuclei that regulate satiety (for review, see Ludwig & Leng, 2006; Sabatier *et al.* 2013). In addition to dendritic release, OT and AVP are released from PVN neuron axonal endings, in a process regulated by the electrical activity of magnocellular neurosecretory cells. Increased electrical activity in magnocellular neurons is thought to induce peptide (OT/AVP) release from axon terminals, whereas dendritic release remains unchanged and depends on activation of intracellular calcium stores (Ludwig *et al.* 2005; for review, see Ludwig & Leng, 2006). Both axonal and dendritic release is also regulated by extrinsic neurotransmitter and neuromodulatory inputs from different brain areas (Ferguson *et al.* 2008; Hazell *et al.* 2012). Recent reports identify the conserved neuropeptide, relaxin-3, as another putative modulator of PVN neuron activity, with significant effects on feeding behaviour in rats (McGowan *et al.* 2005, 2006; Ganella *et al.* 2013*a*; Calvez *et al.* 2015; Lenglos *et al.* 2015).

Relaxin-3 is the ancestral member of the relaxin peptide family, which consists of seven peptides, known for their role in reproduction and cardiovascular physiological processes (Smith *et al.* 2011; Bathgate *et al.* 2013; Halls *et al.* 2015). In humans, there are three relaxin genes, namely *RLN1*, encoding human relaxin 1 (H1), *RLN2*, encoding human relaxin 2 (H2), and *RLN3*, encoding relaxin-3, and four insulin-like peptide genes, encoding insulin-like peptide 3–6 (INSL3–INSL6). Humans and higher primates have all three relaxin genes, whereas in non-primates only two relaxin genes are present, *RLN1* and *RLN3*. The *RLN1* gene product in non-primates, relaxin, is equivalent to the *RLN2* gene product in humans,

relaxin 2 (H2; Bathgate *et al.* 2013). The role of the *RLN1* gene product in higher primates remains unknown, whereas H2 is the major form of relaxin in mammals that circulates in the blood during pregnancy and has an important role in parturition and lactation (Sherwood, 2004). Relaxin also acts within the brain circumventricular organs, having a role in control of water intake and AVP secretion and blood pressure regulation (Weisinger *et al.* 1993). However, roles for relaxin signalling in different brain areas/circuits have not been extensively investigated (see Ma *et al.* 2005).

Four relaxin family peptide receptors (RXFP) have been identified, RXFP1–RXFP4, which are different types of G-protein-coupled receptors (Bathgate *et al.* 2013). In cell-based systems, RXFP1 and RXFP2 stimulation leads to increases in adenylyl cyclase activity and a rise in intracellular cAMP concentrations, as well as activation of the extracellular signal-regulated kinase (ERK) pathway. RXFP3 stimulation, through $G\alpha_{i/o}$-protein coupling, leads to pertussis toxin-sensitive inhibition of forskolin-stimulated cAMP accumulation (Liu *et al.* 2003) and/or pertussis toxin-sensitive phosphorylation of ERK1/2 and other mitogen-activated protein kinases via either a phosphatidylinositol 3-kinase-dependent or a protein kinase C (PKC)-dependent mechanism (van der Westhuizen *et al.* 2007; Bathgate *et al.* 2013).

RXFP4, which is a pseudogene in the rat, is similar to RXFP3 in that it couples to $G\alpha_{i/o}$-proteins, although less is known about the intracellular pathways activated by this receptor and its cognate ligand, INSL5 (Bathgate *et al.* 2013). It has been reported that relaxin binds RXFP1 and RXFP2, whereas relaxin-3 activates its native receptor, RXFP3, but can also bind and activate RXFP1 and RXFP4, which are present in human and mouse brain and peripheral tissues (Bathgate *et al.* 2013). However, apart from a small number of studies, less is known about the effect of activation of these receptors in native tissues and cells, particularly brain neurons (see e.g. Sunn *et al.* 2002; Blasiak *et al.* 2013).

Notably, unlike other members of the relaxin family, relaxin-3 is abundantly expressed within the mammalian brain (Burazin *et al.* 2002; Bathgate *et al.* 2013). A majority of the relaxin-3-synthesizing neurons in the rat brain are located in the nucleus incertus (NI), a structure located immediately caudal to the dorsal raphe nuclei. Other populations of relaxin-3 neurons are present in the pontine raphe nucleus, in an area dorsal to the substantia nigra, and in the ventrolateral/medial periaqueductal grey (Ma *et al.* 2007). The broad network of relaxin-3 fibres within the mammalian brain and the diversity of physiological processes potentially modulated by this peptide led to the proposal that the relaxin-3–RXFP3 system constitutes an ascending arousal system that impacts behavioural state and associated homeostasis. In most brain areas examined, the distribution of relaxin-3-immunoreactive (ir) fibres

and terminals is broadly consistent with the distribution of *RXFP3* mRNA and binding sites in the rat (Ma *et al.* 2007) and mouse (Smith *et al.* 2010). Relaxin-3 fibres are also present in hypothalamic areas closely related to appetite control and hormonal balance (Tanaka *et al.* 2005; Ma *et al.* 2007). Interestingly, some areas appear to be rich in RXFP3 but have a relatively sparse relaxin-3 fibre density. In this regard, the PVN has a very high density of RXFP3 (Ma *et al.* 2007), whereas anterograde neural tract-tracing studies reveal that the PVN region is largely avoided by fibres originating in the major relaxin-3 source in the brain, the NI (Goto *et al.* 2001).

Nonetheless, in a number of studies, acute RXFP3 activation has been consistently shown to increase food intake in satiated adult male rats during the light/inactive phase (McGowan *et al.* 2005; Kuei *et al.* 2007; Haugaard-Kedström *et al.* 2011; Shabanpoor *et al.* 2012). Subchronic intracerebroventricular administration of relaxin-3 produced a significant increase in average daily food intake and a cumulative increase in body weight (McGowan *et al.* 2006; Hida *et al.* 2006). Notably, a similar significant increase in food intake was observed after injections of relaxin-3 into the PVN and supraoptic nucleus, and this effect occurred after both acute and chronic relaxin-3 injections (McGowan *et al.* 2005, 2006). Chronic intra-PVN relaxin-3 injections resulted in changes in plasma leptin (increase) and thyroid-stimulating hormone (decrease), suggesting an inhibitory influence of relaxin-3 on particular PVN neurons (McGowan *et al.* 2006). Importantly, RXFP3 blockade with a specific antagonist reversed the acute RXFP3 activation orexigenic effect (Kuei *et al.* 2007; Haugaard-Kedström *et al.* 2011; Shabanpoor *et al.* 2012). More recent data identified sex-specific effects of central relaxin-3 administration on food intake, highlighting the higher sensitivity of female rats (Calvez *et al.* 2015; Lenglos *et al.* 2015).

In response to local, virally mediated secretion of a selective RXFP3 receptor agonist, R3/I5, within the PVN, we observed a robust reduction in hypothalamic *OT* and *AVP* mRNA levels (50 and 25% decrease relative to control, respectively), which was associated with a significant increase in body weight and daily food intake (Ganella *et al.* 2013*a*). At the same time, mRNA levels of other hypothalamic 'feeding' peptides (neuropeptide Y, agouti-related peptide and pro-opiomelanocortin) were not altered in the hypothalamic samples collected, which points more to a role for OT and AVP in mediating the orexigenic action of relaxin-3–RXFP3 signalling.

However, despite these informative earlier studies highlighting a likely physiological role for relaxin-3–RXFP3 signalling in the regulation of appetite and body weight, the neuronal mechanisms by which this occurs have not been identified. Therefore, the aim of the present study was to explore the influence of the

native relaxin-3 peptide on identified PVN neuron activity *in vitro*, as well as the involvement and localization (pre- or postsynaptic) of RXFP3 in these PVN neuron responses. To address these questions, both native relaxin-3 and a high-affinity, selective RXFP3 receptor agonist [RXFP3 analogue 2 (RXFP3-A2); Shabanpoor *et al.* 2012] were used in patch-clamp electrophysiological recordings, and the neurochemical nature of recorded cells was subsequently examined. Moreover, the influence of native human relaxin (H2) on the electrical activity of PVN neurons was tested. *In situ* hybridization histochemistry was used to localize *RXFP3* mRNA within identified OT- and AVP-positive neurons and to evaluate the proportion of OT and AVP PVN neurons expressing *RXFP3* in defined PVN regions. Immunohistochemical and neural tract-tracing studies were also conducted to map relaxin-3-containing fibres within and in the vicinity of the PVN and to identify the origin of intra-PVN relaxin-3 nerve processes.

## Methods

### Ethical approval

Procedures used in the immunohistochemical, neural tract-tracing and patch-clamp experiments were conducted in accordance with the European Community Council Directive of 24 November 1986 (86/609/EEC) and the Polish Animal Welfare Act of 21 January 2005 and were approved by the 1st Local Ethical Commission (Krakow, Poland). Rats used for *in situ* hybridization histochemistry studies were cared for and handled according to the Canadian *Guide for the Care and Use of Laboratory Animals*, and the protocol was approved by the host institutional animal care committee. All efforts were made to minimize suffering and to reduce the number of rats used. The experiments conducted comply with the policies and regulations of *The Journal of Physiology* (Drummond, 2009).

### Animals

Male Wistar rats were housed in a standard animal facility at the Jagiellonian University or were obtained from the Canadian Breeding Laboratories (St-Constant, QC, Canada) for the *in situ* hybridization studies. Rats were housed in plastic cages lined with wood shavings, maintained on a 12 h–12 h dark–light cycle and fed standard laboratory rat chow in constant environmental conditions (22–23°C, lights on at 08.00 h). For the patch-clamp studies, 4- to 7-week-old rats were used; for the neural tract tracing, 9- to 12-week-old rats were used, and for the *in situ* hybridization and immunohistochemical experiments, 8- to 10-week-old rats were used.

### Electrophysiology

Experiments were performed during the light phase of the light–dark cycle as described by Blasiak *et al.* (2015). In summary, rats ($n = 66$) were decapitated under deep isoflurane anaesthesia, and whole brains were dissected and submerged in ice-cold, low-sodium, high-magnesium artificial cerebrospinal fluid (ACSF) containing (mM): 185 sucrose, 25 $NaHCO_3$, 3 KCl, 1.2 $NaH_2PO_4$, 2 $CaCl_2$, 10 $MgSO_4$ and 10 glucose, pH 7.4; osmolality 290–300 mosmol $kg^{-1}$. Coronal slices (250 $\mu$m thick) containing the PVN were cut on a Leica VT1000S vibrating microtome (Leica Instruments, Heidelberg, Germany), bisected along the third ventricle and transferred for a minimum of 60 min to an incubation chamber containing carbogenated, warm (32°C) ACSF containing (mM): 118 NaCl, 25 $NaHCO_3$, 3 KCl, 1.2 $NaH_2PO_4$, 2 $CaCl_2$, 2 $MgSO_4$ and 10 glucose, pH 7.4; osmolality 290–300 mosmol $kg^{-1}$. After the recovery period, individual slices were placed in the submerged recording chamber, and the tissue was continuously perfused (2 ml $min^{-1}$) with carbogenated, warm ACSF (32°C). The recording chamber was placed on a fixed stage of an Axio Scope FS2 microscope (Zeiss, Gottingen, Germany) equipped with video-enhanced infrared differential interference contrast.

Whole-cell current-clamp recordings were performed with micropipettes pulled from borosilicate glass capillaries (5–7 M$\Omega$; Sutter Instruments, Novato, CA, USA) on a horizontal puller (Sutter Instruments) and filled with a solution containing (mM): 125 potassium gluconate, 20 KCl, 1.3 $MgCl_2$, 4 $Na_2ATP$, 0.4 $Na_3GTP$, 5 EGTA and 10 HEPES, pH 7.3, osmolality 290–300 mosmol $kg^{-1}$. Biocytin (0.1%; Sigma-Aldrich, Schnelldorf, Germany) was also added to the solution for subsequent immunohistochemical detection. In experiments aimed at indicating the involvement of G$\alpha_{i/o}$-protein in the RXFP3-activated intracellular pathway, pertussis toxin was added to the pipette internal solution (1$\mu$g 1ml$^{-1}$).

The calculated liquid junction potential using this solution was 12.9 mV, and data were corrected for this offset. Cell-attached and subsequent whole-cell configurations were obtained using negative pressure delivered through the recording pipette using the ez-gSEAL pressure controller (NeoBiosystem, San José, CA, USA) or by mouth suction. A SEC 05LX amplifier (NPI, Tamm, Germany) and Signal and Spike2 software (Cambridge Electronic Design, Cambridge, UK) were used for data acquisition and further analysis. The output signal was low-pass filtered at 3 kHz and digitized at 20 kHz. Only neurons with steady input resistance, assessed on the basis of a stable amplitude of response to hyperpolarizing current pulses delivered every 30 s throughout the recording, were subjected to analysis. The activity of only one cell per slice was recorded.

After electrophysiological recordings, slices were fixed for 24 h in 4% formaldehyde in PBS and underwent an immunostaining procedure as described by Blasiak *et al.* (2013). After blocking (with 10% normal donkey serum) and a permeabilization step (with 0.6% Triton X-100; Sigma-Aldrich) for 24 h, slices were incubated with mouse anti-OT (1:1000 dilution; ab78364, Abcam, Cambridge, UK) and avidin-fluorescein conjugate (1:200 dilution; 94091, Sigma Aldrich) or with mouse anti-OT (1:1000 dilution), avidin-fluorescein conjugate (1:200 dilution) and rabbit anti-AVP (1:500 dilution; ab39363, Abcam) in PBS with 0.3% Triton X-100 and 2% normal donkey serum. After 48 h, slices were washed and incubated in anti-mouse Alexa Fluor 647 (1:400 dilution; 715-606-150, Jackson ImmunoResearch, WestGrove, PA, USA) and anti-rabbit CY3-conjugated (1:400 dilution; 711-165-152, Jackson ImmunoResearch) antisera for 24 h. Stained slices were mounted on glass slides, coverslipped with Vectashield containing 4′, 6-diamidino-2-phenylindole (DAPI) (Vector Laboratories, Peterborough, UK), and examined using an Axio Observer Z1 confocal laser microscope (Zeiss).

### Peptides and drugs

The ACSF and intrapipette ingredients, pertussis toxin and cadmium chloride were purchased from Sigma-Aldrich. All drugs and peptides were dissolved in ACSF and applied directly through the bath perfusion system. Tetrodotoxin citrate (TTX), bicuculline methiodide, 2-amino-5-phosphopentanoic acid (AP5) and 6-cyano-7-nitroquinoxaline-2,3-dione (CNQX) disodium salt were purchased from Tocris Bioscience (Bristol, UK). The RXFP3 agonist, RXFP3-A2 {[R3A(11–24,C15→A)B]} was synthesized using solid-phase peptide synthesis and purified using reverse-phase HPLC (The Florey Institute of Neuroscience and Mental Health, Victoria, Australia; Shabanpoor *et al.* 2012) and supplied by M. Akhter Hossain (The Florey Institute of Neuroscience and Mental Health). The RXFP3 antagonist, R3 B1-22R, was kindly provided by K. Johan Rosengren (The University of Queensland, Queensland, Australia; Haugaard-Kedström *et al.* 2011). H2 Relaxin was kindly provided by Ross A. D. Bathgate (The Florey Institute of Neuroscience and Mental Health). Relaxin-3 was purchased from Phoenix Pharmaceuticals (Karlsruhe, Germany).

### Double-labelling immunohistochemistry and *in situ* hybridization histochemistry

Rats ($n = 6$) were anaesthetized I.P. (60 mg kg$^{-1}$ ketamine, Vetoquinol, Lavaltrie, QC, Canada; plus 7.5 mg kg$^{-1}$ xylazine, Bimeda, Cambridge, ON, Canada) and perfused transcardially with 200 ml of saline followed by 500 ml of 4% paraformaldehyde solution. Brains were

removed at the end of the perfusion and postfixed in paraformaldehyde for 1 week. Brains were then transferred to a solution containing 4% paraformaldehyde and 20% sucrose for 12 h before being cut at 30 $\mu$m thickness in the coronal plane using a sliding microtome (HM440E; Microm International GmbH, Walldorf, Germany).

Immunohistochemical detection of AVP or OT was combined with detection of *RXFP3* mRNA by *in situ* hybridization histochemistry to determine whether AVP or OT neurons express *RXFP3* mRNA according to an established method (Timofeeva *et al.* 2005). Serial coronal brain sections were first processed for immunohistochemistry using a conventional avidin–biotin–immunoperoxidase method. Briefly, brain sections were washed in sterile 50 mM potassium phosphate-buffered saline (KPBS; pH 7.2) pretreated with diethyl pyrocarbonate and blocked for endogenous peroxidase activity by 30 min incubation in 3.3% $H_2O_2$ diluted in methanol. Sections were then rinsed in KPBS and incubated overnight at 4°C with anti-AVP (1:10,000 dilution; 20069, Immunostar, Hudson, WI, USA) or anti-OT (1:1000; 20068, Immunostar) antibody diluted in KPBS (50 mM) with Triton X-100 (0.4%) and bovine serum albumin (0.4%). Thereafter, sections were incubated for 60 min with biotinylated goat anti-rabbit IgG (1:1500 dilution; Vector Laboratories, Burlington, ON, Canada) followed by a 60 min incubation with avidin–biotin–peroxidase (ABC) complex (Vectastain ABC Elite Kit; Vector Laboratories). After several rinses in Tris-imidazole buffer (pH 7.2), the brain sections were allowed to react in a mixture containing the chromogen 3,3′-diaminobenzidine tetrahydrochloride (0.05%) and 1% hydrogen peroxide. Thereafter, brain sections were rinsed in KPBS, mounted onto poly L-lysine-coated slides and fixed in 4% paraformaldehyde for 20 min, digested for 25 min at 37°C with proteinase K (10 $\mu$g ml$^{-1}$), acetylated with acetic anhydride (0.25%), and dehydrated through graded concentrations of ethanol. Sections were incubated overnight with antisense $^{35}$S-labelled cRNA probes ($10^7$ c.p.m. ml$^{-1}$) for *RXFP3* (generated from a 907 bp fragment including a 274–1180 bp sequence of the complete 1431 bp rat *RXFP3* cDNA; GenBank NM_001008310; Lenglos *et al.* 2014) at 60°C. Thereafter, slides were rinsed with sodium chloride–sodium citrate solution, digested with ribonuclease-A (20 $\mu$g ml$^{-1}$), and dehydrated through an ethanol gradient. The slides were defatted in toluene and exposed for 3 weeks to nuclear emulsion (Eastman Kodak, Rochester, NY, USA).

The presence of neurons positive for peptide immunoreactivity (brown staining) and *RXFP3* mRNA hybridization signal (silver grains) was assessed bilaterally in two coronal brain sections per rat in the ventral part (PaV), medial parvocellular part (PaMP), lateral magnocellular part (PaLM) and dorsal cap (PaDC) of the PVN from 1.72 to 1.80 mm caudal to bregma

(Paxinos & Watson, 2007), using an Olympus BX61 microscope (Olympus Canada, Richmond Hill, ON, Canada) equipped with a DVC-2000C digital camera (DVC Company Inc., Austin, TX, USA).

### Immunohistochemistry and neural tract tracing

For the immunohistochemical detection of relaxin-3 fibres and OT and AVP neurons within the area of the PVN, rats ($n = 5$) were anaesthetized with pentobarbital (240 mg kg$^{-1}$, I.P.; Vetbutal; Biowet, Pulawy, Poland) and killed by transcardial perfusion with 300 ml of saline followed by 300 ml of 4% formaldehyde in PBS (made fresh from paraformaldehyde; Sigma-Aldrich). Brains were removed from the skull and after 24 h postfixation, coronal sections (40 $\mu$m thick) were cut on a Leica VT1000S vibrating microtome (Leica Instruments). After perfusion, brain preparation and washing, tissue sections containing PVN were incubated for 48 h at 4°C in PBS with mouse anti-relaxin-3 (1:50 dilution; The Florey Institute of Neuroscience and Mental Health; Tanaka *et al.* 2005) and subsequently, after washing, sections were incubated overnight at 4°C with anti-mouse Alexa Fluor 488 (1:200 dilution; 715-545-150, Jackson ImmunoResearch) secondary antibody. After washing, slices were incubated for 48 h at 4°C in PBS with mouse anti-OT (1:5000 dilution) and rabbit anti-AVP (1:1,000) antibody. After washing, brain sections were incubated for 18 h with anti-mouse Alexa Fluor 647 and anti-rabbit CY3. Sections were finally mounted on glass slides, coverslipped with Fluoroshield (Sigma-Aldrich) and examined using a confocal laser microscope (LSM 710 on Axio Observer Z1 microscope; Zeiss).

Reconstruction of the distribution of relaxin-3 fibres in the area of the PVN and OT and AVP cell bodies within the PVN was based on a series of seven projections made from z-stacks (2928 × 2928 pixels, acquired using a 20×/0.5 Plan-Neofluar objective with the 0.6× digital zoom) combined into one image using ImageJ (National Institutes of Health, Bethesda, MD, USA). The distance from bregma was assessed by matching the tissue to the corresponding plate of a stereotaxic atlas of rat brain (Paxinos & Watson, 2007).

For neural tracer injections, adult male Wistar rats (300 g; $n = 3$) were treated as described by Blasiak *et al.* (2015). Under deep isoflurane anaesthesia, retrograde tracer (undiluted red fluorescent RetroBeads; LumaFluor, Naples, FL, USA) was injected into the PVN magnocellular part, using the following stereotaxic co-ordinates; anteroposterior −1.7 mm, mediolateral 0.4 mm and dorsoventral −7.8 mm from bregma (Paxinos & Watson, 2007). Tracer injections were performed using microinjection needles pulled from borosilicate glass capillaries (Sutter Instruments) to a fine tip of 30 $\mu$m using a vertical micropipette puller (PE-21; Narishige,

Tokyo, Japan). The injected volume was controlled using a Hamilton syringe (1 $\mu$l; Hamilton, Bonaduz, Switzerland) connected to the microinjection needle. After 7 days of recovery, rats were again anaesthetized and underwent a unilateral injection of colchicine (0.5 mg in 5 $\mu$l of 0.9% NaCl; Sigma-Aldrich) into the lateral cerebral ventricle (anteroposterior −0.7 mm, mediolateral 1.8 mm and dorsoventral −4.0 mm from bregma) in order to improve the detection of somatic relaxin-3 immunoreactivity. After 24 h, similar perfusion and staining procedures to those used for immunohistochemical detection of relaxin-3 fibres were conducted. Only brains with injections confined to the magnocellular part of the PVN were processed further and included in the analysis.

Brain sections (40 $\mu$m thick) containing all known relaxin-3-synthesizing regions (periaqueductal grey, area dorsal to substantia nigra, raphe pontis and nucleus incertus) were incubated for 1 h in 10% normal donkey serum with 0.3% Triton X-100. Subsequently, the sections were incubated for 48 h at 4°C in PBS containing mouse anti-relaxin-3 [1:50 dilution; The Florey Institute of Neuroscience and Mental Health; monoclonal cell line originally supplied by the International Patent Organism Depository (IPOD) National Institute of Advanced Industrial Science and Technology (AIST), Tsukuba, Ibaraki, Japan; see Tanaka *et al.* 2005; Ma *et al.* 2013] and then, after washing, for 18 h at 4°C with secondary anti-mouse Alexa Fluor 647 antibodies. The sections were mounted on glass slides and coverslipped with Fluoroshield (Sigma-Aldrich). Images were collected using a confocal laser microscope (LSM 710 on Axio Observer Z1 microscope; Zeiss).

### Data analysis and statistics

A custom MATLAB script (MathWorks Inc., Natick, MA, USA) was used for the analysis of electrophysiological data. The change in recorded signal in response to the peptide application was considered significant if it differed from the baseline by more than three standard deviations. In recordings where an inhibitory effect of a peptide on spontaneously firing neurons was observed, quiescence/complete cessation of action potential firing was defined as the time period during which no action potential was observed for a minimum of 60 s of the recording. The data were analysed with Fisher's exact test, or the Wilcoxon matched pairs signed rank test, according to the result of the D'Agostino and Pearson omnibus normality test. All tests were two tailed. The application of a particular test is indicated in the Results. All values are provided as mean ± SD. Data were considered to be significantly different at $P < 0.05$. Statistical analysis was performed using GraphPad Prism version 6.00 for Windows (GraphPad Software Inc., La Jolla, CA, USA).

# Results

## Electrophysiological determination of recorded PVN cell types

Paraventricular nucleus neurons can be divided into two types based on their distinct electrophysiological properties. Type I putative magnocellular neurons display a transient outward rectification originating from an outward transient inactivating A-type potassium current and a lack of low-threshold calcium spikes. Type II putative parvocellular neurons are characterized by the lack of transient outward rectification and common occurrence of low-threshold spikes caused by a T-type calcium current (Luther & Tasker, 2000). According to these characteristics, in the present study 138 putative magnocellular and 46 putative parvocellular PVN neurons were tested in electrophysiological experiments.

## Paraventricular nucleus neurons are sensitive to RXFP3 activation

In total, the responsiveness to the selective RXFP3 agonist, RXFP3-A2 (600 nM), of 138 PVN neurons was tested in whole-cell patch-clamp recordings with the standard solution in the recording pipette. Based on their electrophysiological characteristics, 98 neurons tested with RXFP3-A2 were classified as type I putative magnocellular and 40 as type II putative parvocellular neurons (Fig. 1). Overall, in all experimental conditions, 82% of type I neurons (80 of 98 cells) and 40% (16 of 40) of type II putative parvocellular PVN neurons were inhibited by RXFP3-A2 (Figs 2 and 3).

## RXFP3 activation inhibits type I PVN neuron spontaneous activity

In normal ACSF, RXFP3-A2 (600 nM) inhibited 81% (59 of 73) of the type I PVN neurons examined. Among neurons sensitive to the agonist, 55 cells spontaneously generated action potentials, and RXFP3-A2 application resulted in either complete cessation of firing ($n = 18$; Fig. 2A) or a decrease in the mean firing frequency ($n = 37$, from 7.9 ± 4.4 to 4.2 ± 3.6 Hz; Fig. 2E). Four type I neurons sensitive to RXFP3-A2 were quiescent, and exposure to the agonist peptide evoked membrane hyperpolarization in these cells (from −67.3 ± 8.1 to −71.7 ± 7.0 mV; Fig. 2B). In 29% (17 of 59) of RXFP3-A2-sensitive cells, the input resistance decreased in the presence of RXFP3-A2 by 107.1 ± 66.7 MΩ (from 549.9 ± 209.7 to 442.8 ± 188.6 MΩ).

The spiking activity of 16% (12 of 73) of the type I PVN neurons was not affected by RXFP3-A2 in normal ACSF, and the frequency of firing of two of 73 tested cells increased after RXFP3-A2 application (from 11.9 ± 4.9 to 15.8 ± 6.7 Hz; Fig. 2E).

The specificity of the effects of the RXFP3-A2 agonist was verified using the selective RXFP3 antagonist, R3 B1-22R (Haugaard-Kedström *et al.* 2011). Three spontaneously quiescent and four spiking neurons inhibited by RXFP3-A2 (membrane potential change −3.13 ± 0.45 mV, $n = 3$; spiking frequency change −4.11 ± 1.16 Hz, $n = 4$) were subsequently exposed to the agonist in the presence of 20 μM R3 B1-22R. The inhibitory action of RXFP3-A2 was blocked in the presence of the antagonist (membrane potential change 0.37 ± 0.71 mV, $n = 3$; spiking frequency change −0.48 ± 0.89 Hz, $n = 4$; Fig. 2A and B). Importantly, the action of R3 B1-22R was reversible, because after antagonist washout, the hyperpolarizing effect of RXFP3-A2 was again observed ($n = 5$; Fig. 2B and G).

The antagonist itself depolarized four tested neurons, causing an increase in spiking frequency (from 6.8 ± 2.8 to 10.85 ± 3.25 Hz; Figs 2A).

## Type I PVN neurons express functional RXFP3

Twenty-two type I PVN neurons inhibited by RXFP3-A2 (600 nM) in normal ACSF were subsequently exposed to the agonist peptide in the presence of TTX (1 μM). In 95% of cells (21 of 22 neurons tested), the presence of TTX did not prevent the hyperpolarizing action of RXFP3-A2 (Fig. 2C). Recorded PVN neurons were hyperpolarized by 2.9 ± 0.7 mV (from −59.6 ± 7.9 to −62.6 ± 7.7 mV).
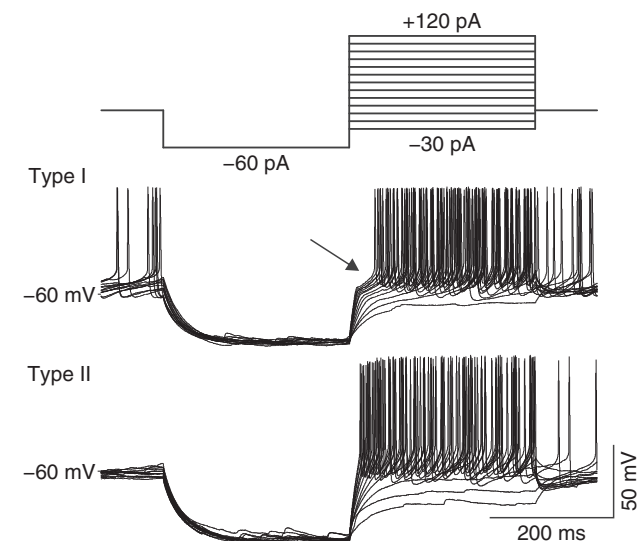


**Figure 1. Electrophysiological characteristics of paraventricular nucleus (PVN) neurons**
Different types of PVN neurons are distinguished by their response to incremental depolarizing pulses delivered at a hyperpolarized potential (top trace). Type I putative magnocellular neurons express a transient outward rectification caused by $I_A$ potassium current reflected as a delay in the onset to the first action potential (arrow). Type II putative parvocellular neurons lack the outward rectification and delay in response to the same current stimuli.
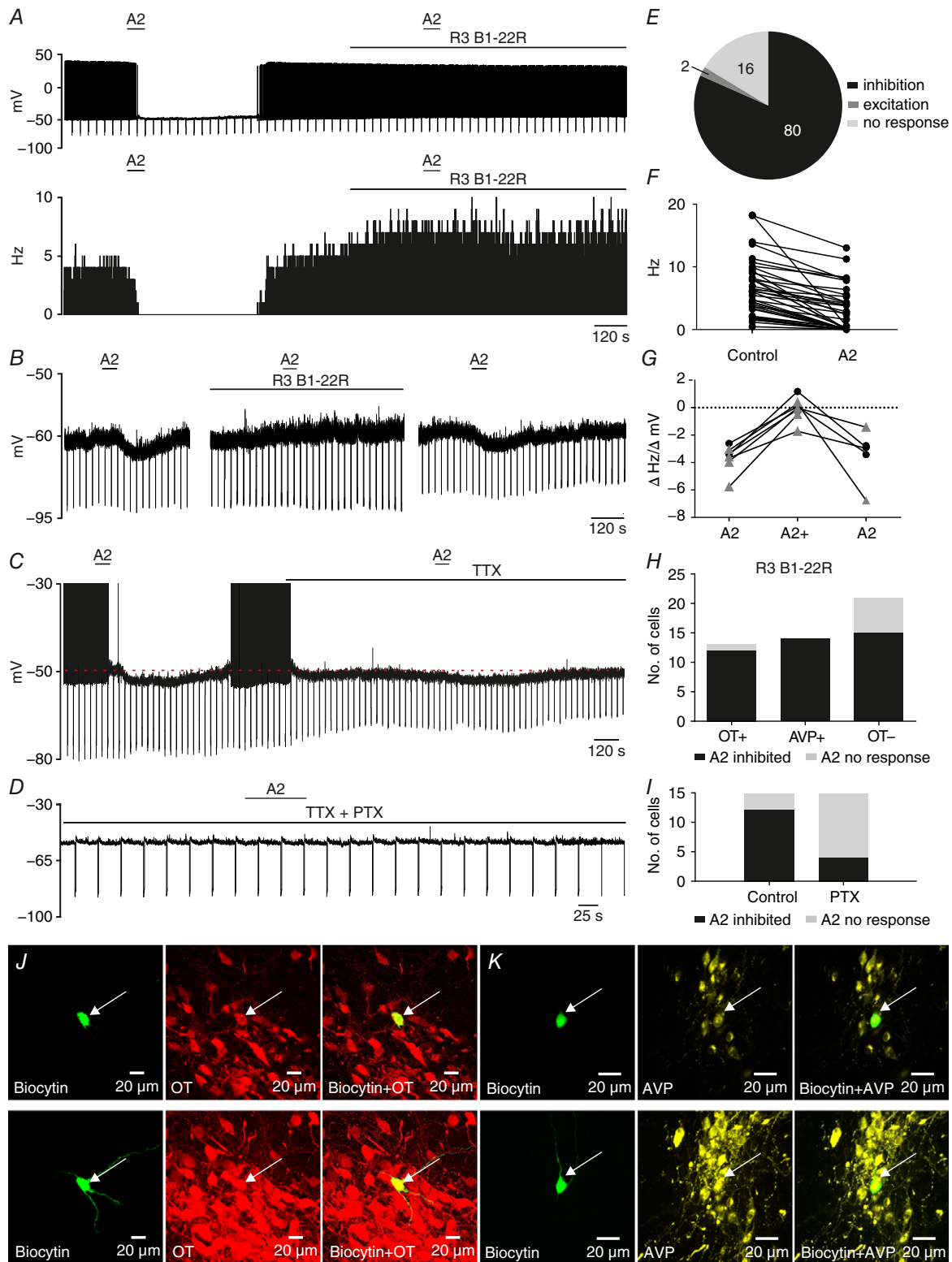
**Figure 2. RXFP3 activation inhibits type I putative magnocellular PVN neurons**

*A*, representative trace of a zero current-clamp recording illustrating the inhibitory action of RXFP3-A2 application (A2; 600 nм; horizontal bar) on spontaneous firing (upper trace) of a type I PVN neuron and blockade of the RXFP3-A2 action by the RXFP3 antagonist, R3 B1-22R (20 μм; horizontal bar) in normal artificial cerebrospinal fluid (ACSF). Lower trace, corresponding activity histogram; bin, 1 s. *B*, representative trace of spontaneously quiescent type I PVN neuron illustrating the hyperpolarizing effect of RXFP3-A2 agonist (left, horizontal bar),

the blockade of RXFP3-A2 action by the presence of R3 B1-22R antagonist (middle, horizontal bar) and the return of the inhibitory RXFP3-A2 effect after antagonist washout (right). C, the inhibitory effect of RXFP3-A2 (600 nM; horizontal bar) observed in the ACSF (action potentials were truncated at −30 mV) persists in the presence of TTX (0.5 μM; horizontal bar). Downward deflections represent voltage responses of the recorded neuron to hyperpolarizing current injections. D, typical trace illustrating lack of hyperpolarizing action of RXFP3-A2 agonist (A2; 600 nM; horizontal bar) when applied in the presence of pertussis toxin, an irreversible inhibitor of $G\alpha_{i/o}$-proteins (PTX; 1 μg ml$^{-1}$) in the recording pipette. E, pie chart illustrating the number of type I PVN neurons responding in different ways to RXFP3-A2 application. F, inhibitory effect of RXFP3-A2 on firing frequency of type I PVN neurons. G, reversible blockade of RXFP3-A2 effect by R3 B1-22R. Black circles represent the change in membrane potential, and grey triangles represent the change in firing frequency, recorded in spontaneously quiescent and firing neurons, respectively. H, number of different type I PVN neuronal populations identified by postrecording immunohistochemical staining and their sensitivity to RXFP3-A2 application. OT+ and AVP+, oxytocin- and arginine-vasopressin-positive cells, respectively, identified by double staining; OT− are neurons identified as lacking oxytocin immunoreactivity after anti-OT single staining procedure. I, number of magnocellular PVN neurons unaffected and inhibited by RXFP3-A2 in control recordings and in experiments with PTX (1 μg ml$^{-1}$) in the recording pipette. J, top panels, confocal images of a single optical slice (1 μm) of a type I PVN neuron inhibited by RXFP3-A2 (arrow). Left, biocytin-filled neuron (green); middle, OT-immunoreactivity; and right (red), merged image indicating that the recorded neuron was immunopositive for oxytocin. Bottom panels, confocal projection images (1 μm optical slice) of neuron shown in top panels. K, top panels, confocal images of single optical slice (1 μm) of another type I PVN neuron inhibited by RXFP3-A2 (arrow). Left, biocytin-filled neuron (green); middle, AVP immunoreactivity (yellow); and right, merged image indicating that the recorded neuron was immunopositive for AVP. Bottom panels, confocal projection images (1 μm optical slice) of neuron shown in upper trace. [Colour figure can be viewed at wileyonlinelibrary.com]

In order to examine the possible action of RXFP3-A2 on glutamate and GABA release from presynaptic terminals within the PVN (Boudaba *et al.* 2003), 22 type I neurons were tested for sensitivity to RXFP3-A2 (600 nM) in the presence of TTX (1 μM) and glutamate and GABA receptor antagonists (50 μM AP-5, 10 μM CNQX and 20 μM bicuculline). In 21 of 22 type I PVN neurons tested in the presence of TTX and glutamate/GABA receptor antagonists, RXFP3-A2 evoked membrane hyperpolarization by 2.5 ± 1.3 mV (from −59.5 ± 8.6 to −61.9 ± 8.9 mV).

### RXFP3 stimulation inhibits PVN magnocellular neurons via a $G\alpha_{i/o}$-protein-dependent pathway

In a separate set of experiments, the pipette recording solution was supplemented with pertussis toxin (PTX; 1 μg ml$^{-1}$), an irreversible inhibitor of $G\alpha_{i/o}$-proteins. All recordings were conducted in the presence of TTX (1 μM) in the ACSF. At a minimum of 900 s after whole-cell configuration initiation, RXFP3-A2 agonist (600 nM) was applied via the bathing solution. In 11 of 15 type I PVN neurons tested, RXFP3-A2 application failed to hyperpolarize tested neurons (Fig. 2D and I). Only four neurons (27%) recorded with recording solution that contained PTX were hyperpolarized by RXFP3-A2 by −2.97 ± 0.9 mV. At the same time, control neurons that were recorded with the standard intrapipette solution (n = 15) in the presence of TTX were hyperpolarized by RXFP3-A2 application in 80% of cases (n = 12, mean difference −3.3 ± 0.6 mV). The proportion of cells responsive to RXFP3-A2 in TTX and in the presence of PTX was significantly different (P = 0.009, Fisher's exact test).

### RXFP3 activation induces a calcium-dependent outward current

In studies to further our understanding of the influence of RXFP3 activation on PVN neurons, neurons responsive to RXFP3-A2 (600 nM) in ACSF containing TTX (controls for the PTX experiments) were subsequently re-exposed to the agonist peptide in an ACSF/TTX bathing solution enriched with CdCl$_2$ (200 μM), a non-specific voltage-sensitive calcium channel blocker (Hille, 2001). Only neurons in which membrane potential and input resistance remained stable after the first agonist application were tested. To investigate changes in the whole-cell current, voltage ramp tests (600 ms, from −140 to 20 mV) were performed during baseline and maximal response to the agonist (or expected response time) in both ACSF/TTX and ACSF/TTX/CdCl$_2$ solutions. In all tested type I PVN neurons, the whole-cell I–V relationship was outwardly rectifying, as previously reported (Bourque, 1986; Fig. 4). RXFP3 activation induced an outward current that was sensitive to external CdCl$_2$, because CdCl$_2$ abolished (n = 5) or attenuated (n = 2) the RXFP3-A2-induced outward current and membrane hyperpolarization (n = 7, from −5.2 ± 1.5 to 0.4 ± 0.6 mV, change in membrane potential in control and in the presence of CdCl$_2$, P = 0.03, Wilcoxon matched-pairs signed rank test; Fig. 4).

### Oxytocin and vasopressin type I PVN neurons are responsive to RXFP3 agonist

Brain slices examined for the effects of RXFP3-A2 in patch-clamp recordings were subsequently stained immunohistochemically for OT and AVP in single- (OT) or double-staining procedures (OT + AVP). Among 48

successfully stained slices, 13 neurons were OT positive (Fig. 2*J*), 14 were AVP positive (Fig. 2*K*) and 21 were OT negative. Importantly, 92% of OT-ir neurons (12 of 13 cells) were hyperpolarized by RXFP3-A2 agonist, and all 14 AVP-ir neurons were inhibited by RXFP3-A2 in preceding electrophysiological recordings. Twenty-one neurons stained for potential OT-ir were identified as OT negative. Within this group, 71% (15 cells) were hyperpolarized by RXFP3-A2 and 29% (6 cells) were not affected by the RXFP3 agonist (Fig. 2*H*).

### Type II neurons are sensitive to RXFP3 activation

A significantly smaller proportion of type II putative parvocellular PVN neurons was inhibited by RXFP3-A2 than type I putative magnocellular neurons (40%, 16/40 of type II *vs* 82%, 80/98 of type I PVN neurons tested, $P < 0.0001$, Fisher's exact test; Fig. 3*B*). Similar to the effect on type I neurons, the inhibitory action of RXFP3-A2 on

spontaneously active type II PVN neurons was manifested as either complete blockade of action potential firing ($n = 3$) or a decrease in the frequency of spontaneous firing ($n = 11$, from $5.2 \pm 2.2$ to $2.9 \pm 2.6$ Hz; Fig. 3*A* and *C*). Two neurons sensitive to RXFP3-A2 were quiescent, and agonist application caused membrane hyperpolarization in these cells. In four type II neurons, input resistance was decreased by $41.2 \pm 23.5$ MΩ ($375.1 \pm 120.6$ MΩ before *vs* $333.9 \pm 102.2$ MΩ) in the presence of RXFP3-A2. Three type II cells were excited in normal ACSF by RXFP3-A2 application (from $2.2 \pm 1.6$ to $3.6 \pm 1.7$ Hz). In the remaining 21 putative parvocellular PVN neurons, RXFP3-A2 had no effect on recorded electrical activity (Fig. 3*B*).

Immunohistochemical staining of type II PVN neurons, previously tested in patch-clamp recordings, revealed that the majority of type II cells were OT or AVP negative (11 of 13 neurons). From 13 slices stained against OT and AVP, two neurons were OT-ir (Fig. 3*D*) and none of the neurons
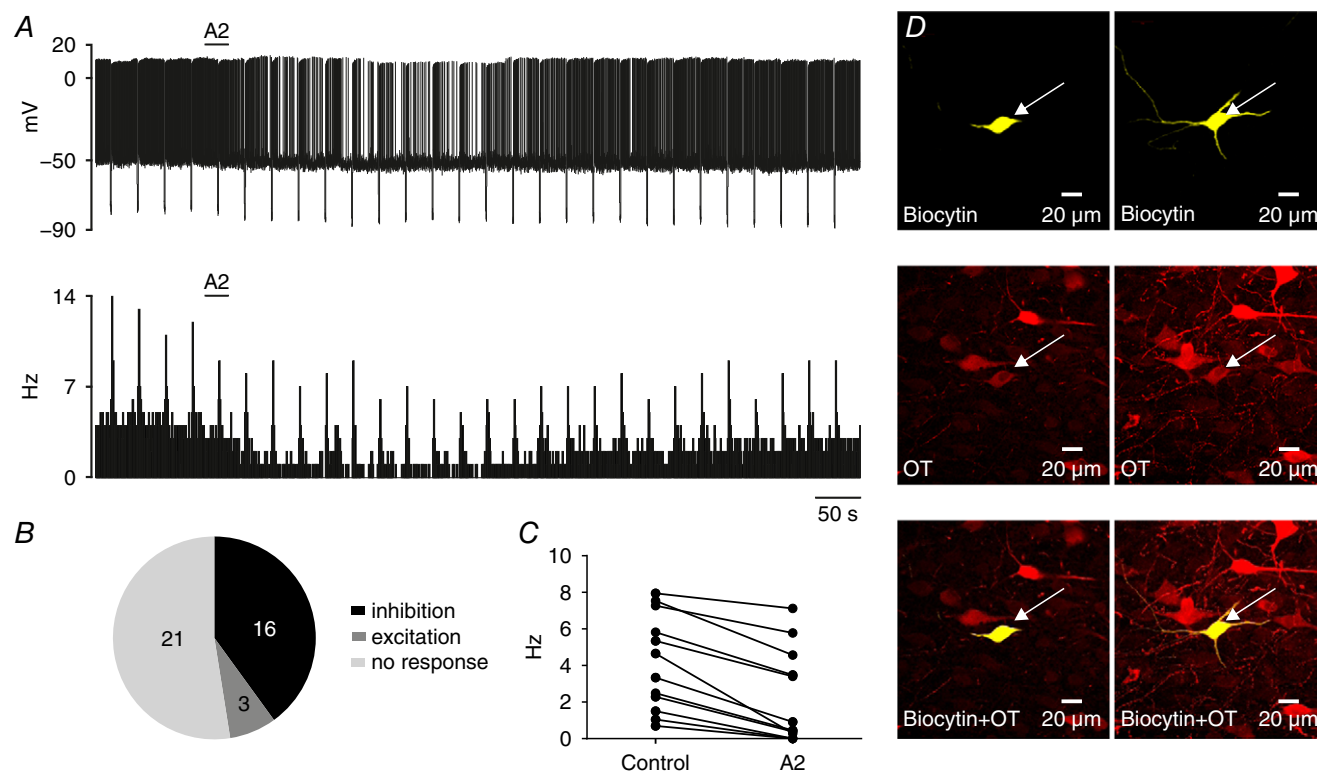


**Figure 3. RXFP3 activation inhibits a population of type II putative parvocellular PVN neurons**
*A*, representative trace of a zero current-clamp recording (upper) and corresponding activity histogram (lower; bin, 1 s) of a spontaneously active type II PVN neuron, illustrating the inhibitory effect of RXFP3-A2 application (A2; 600 nM; horizontal bar) in normal ACSF. Downward deflections correspond to voltage responses of the recorded neuron to hyperpolarizing current injections. *B*, number of type II PVN neurons responding in different ways to RXFP3-A2 application. *C*, inhibitory effect of RXFP3-A2 on firing frequency of type II PVN neurons. *D*, left panels, confocal images of a single optical slice (1 μm) of a type II PVN neuron inhibited by RXFP3-A2, indicated by arrow. Top, biocytin-filled neuron (yellow); middle, OT immunoreactivity (red); and bottom, merged image illustrating that the recorded neuron was immunopositive for OT. Right panels, confocal projection images (1 μm optical slice) of neuron shown on the left. [Colour figure can be viewed at wileyonlinelibrary.com]

was identified as AVP-ir. Both of the identified OT-ir neurons were hyperpolarized by RXFP3-A2 application in normal ACSF. Among 11 OT- or AVP-negative neurons, three were hyperpolarized and seven were not affected by RXFP3-A2.

### Oxytocin and AVP PVN type I neurons are directly sensitive to native relaxin-3 peptide

The influence of relaxin-3 peptide (100 nM) was tested on 25 type I PVN neurons under zero current-clamp mode (14 in normal ACSF and 11 in the presence of TTX and glutamate and GABA receptor antagonists). Overall, relaxin-3 hyperpolarized 92% of type I neurons (23 of 25 cells). In normal ACSF, 86% of PVN neurons (12 of 14) were inhibited by relaxin-3 application (Fig. 5*A* and *D*).

This inhibition was manifested as a complete cessation of firing ($n = 9$) or a reduction in spiking frequency ($n = 3$, from $6.9 \pm 1.9$ to $4.4 \pm 1.5$ Hz). The input resistance of nine cells was reduced by $209.8 \pm 328.5$ MΩ (from $814.4 \pm 616.6$ to $604.6 \pm 347.4$ MΩ). Importantly, the hyperpolarizing action of relaxin-3 (100 nM) was blocked by the presence of the RXFP3 antagonist, R3 B1-22R ($n = 4$; Fig. 5*A*). In three of these neurons, relaxin-3 administration in the presence of RXFP3 antagonist caused an increase in firing frequency (from $5.3 \pm 1.3$ to $8.9 \pm 2.0$ Hz).

Another group of type I PVN neurons ($n = 11$) was tested for responsiveness to application of relaxin-3 (100 nM) in ACSF containing TTX and glutamate and GABA receptor antagonists (Fig. 5*C* and *E*). In 91% of neurons recorded in these conditions ($n = 10$), relaxin-3
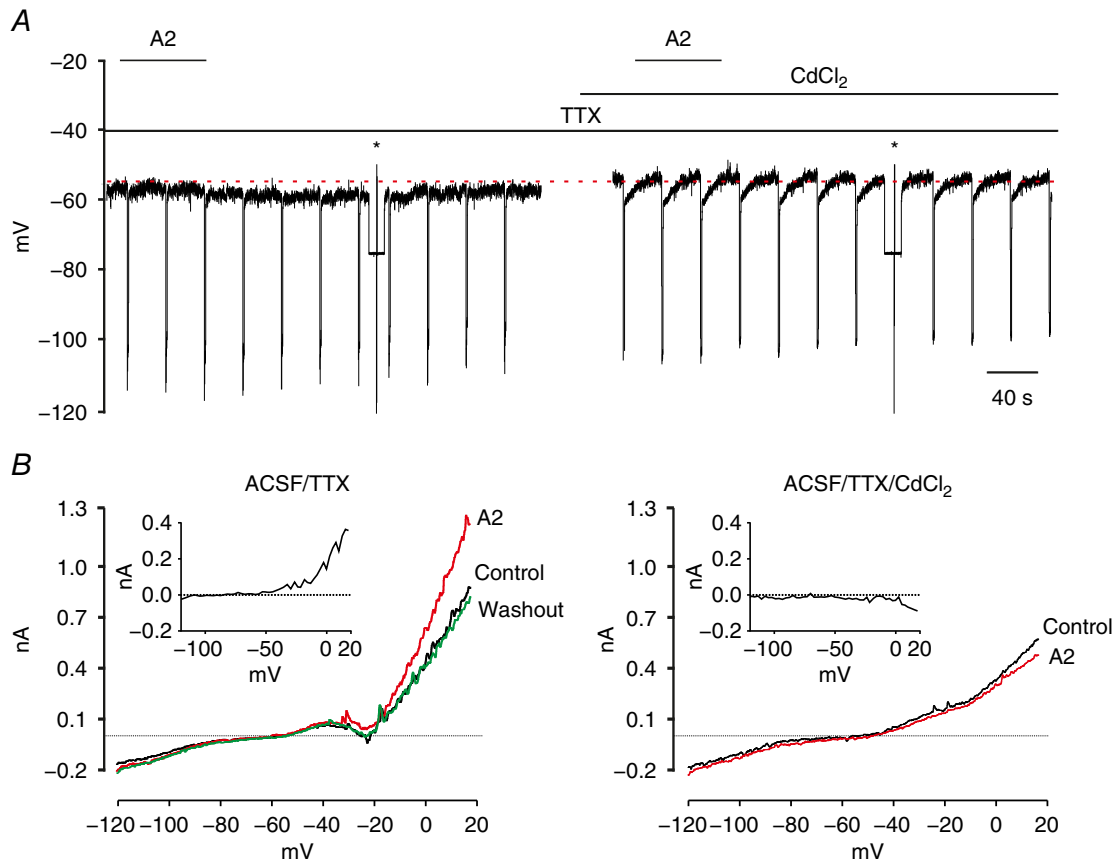


**Figure 4. RXFP3 activation induces cadmium-sensitive whole-cell outward current**
*A*, representative trace of a zero current-clamp recording illustrating the hyperpolarizing effect of bath-applied RXFP3-A2 agonist (A2; 600 nM; horizontal bar) on the membrane potential in ACSF supplemented with TTX (1 μM; left) and a lack of hyperpolarizing action (on the same cell) when the agonist was applied in ACSF/TTX containing CdCl$_2$ (200 μM). Asterisks indicate the time of ramp tests in voltage-clamp mode illustrated in *B*. *B*, current traces recorded in response to voltage ramp tests (600 ms, from −140 to 20 mV) in ACSF/TTX (left) and during perfusion of slices with ACSF/TTX/CdCl$_2$ (right) in control conditions and with application of RXFP3-A2 agonist. Insets, outward difference current induced by RXFP3-A2 agonist, calculated by subtracting the control current from that recorded during application of RXFP3-A2 agonist. Abbreviations: ACSF/TTX, artificial cerebrospinal fluid with 1 μM tetrodotoxin; and ACSF/TTX/CdCl$_2$, artificial cerebrospinal fluid with 1 μM tetrodotoxin and cadmium chloride (200 μM). [Colour figure can be viewed at wileyonlinelibrary.com]
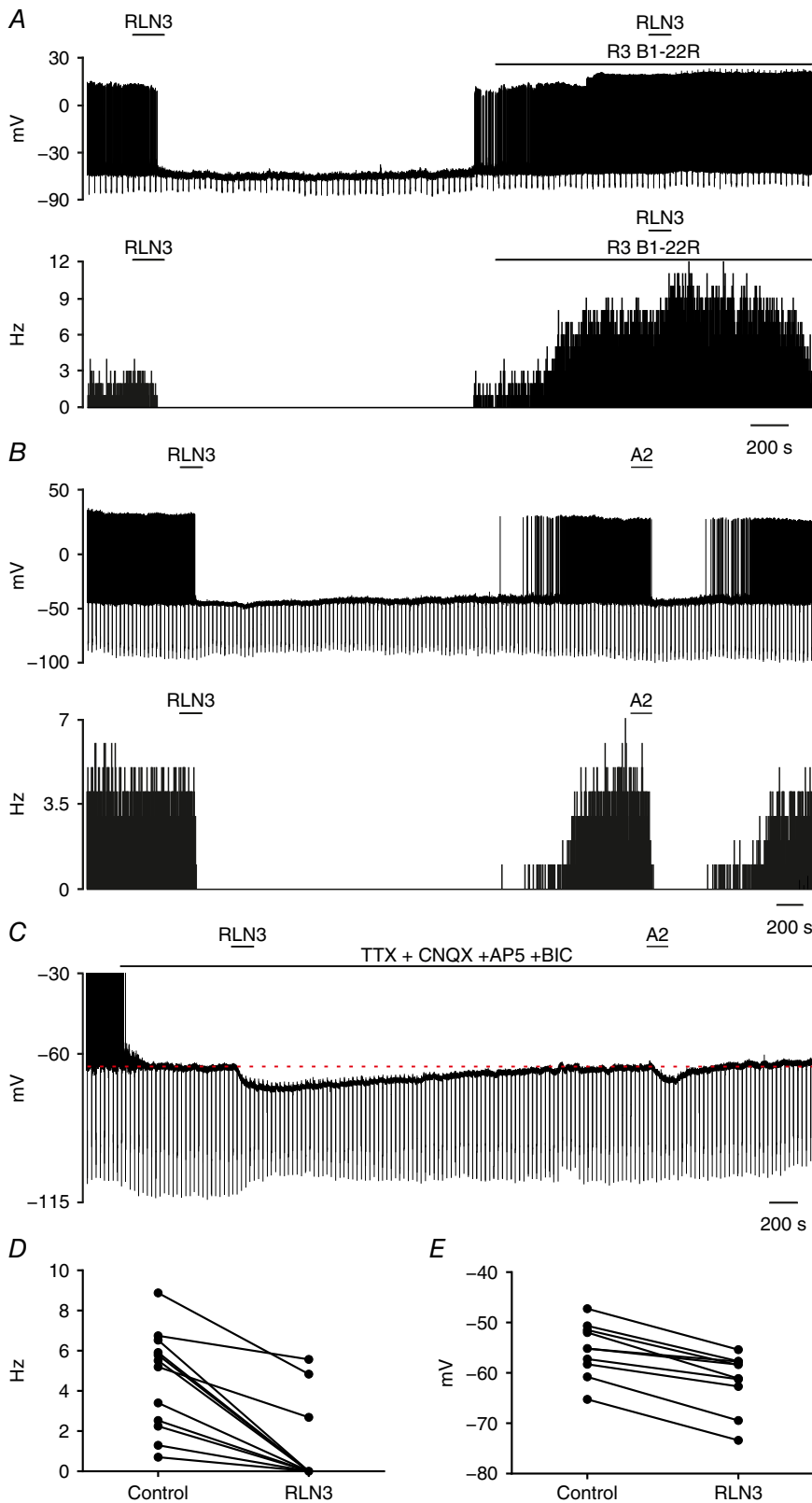
**Figure 5. Relaxin-3 inhibits type I PVN neurons via RXFP3**

*A*, representative trace of a zero current-clamp recording (upper) and corresponding activity histogram (lower; bin, 1 s) of a spontaneously active type I PVN neuron inhibited by relaxin-3 (100 nM; horizontal bar) and blockade of relaxin-3 action by the RXFP3 antagonist, R3 B1-22R (20 μM; horizontal bar). Note an increase of firing in the presence of the RXFP3 antagonist. *B* and *C*, representative traces of a zero current-clamp recording illustrating the inhibitory effect of relaxin-3 (100 nM; horizontal bar) and RXFP3-A2 application (600 nM; horizontal bar) on a single type I PVN neuron in normal ACSF (*B*) and in the presence of a cocktail of TTX (1 μM), 2-amino-5-phosphopentanoic acid (AP-5; 50 μM), 6-cyano-7-nitroquinoxalene-2,3-dione (CNQX; 10 μM) and bicuculline (20 μM) (*C*), indicating the postsynaptic action of both peptides (action potentials were truncated at −30 mV). *D*, inhibitory effect of relaxin-3 on firing frequency of type I PVN neurons. *E*, inhibitory effect of relaxin-3 on membrane potential of type I PVN neurons in the presence of TTX, AP-5, CNQX and bicuculline. [Colour figure can be viewed at wileyonlinelibrary.com]

evoked membrane hyperpolarization by $6.2 \pm 2.4$ mV (from $-55.3 \pm 5.3$ to $-61.5 \pm 5.7$ mV), which indicates its direct, postsynaptic action.

After electrophysiological recordings, neurons tested for responsiveness to relaxin-3 were stained for OT and AVP. Amongst 16 successfully stained neurons, six were classified as OT positive and 10 as AVP positive. All PVN neurons double labelled against biocytin and OT or biocytin and AVP were hyperpolarized by relaxin-3 during previous patch-clamp recordings.

### Type I PVN neurons are directly sensitive to both relaxin-3 and selective RXFP3 agonist

Twelve neurons tested with relaxin-3 were subsequently exposed to the selective RXFP3 agonist, RXFP3-A2, in normal ACSF ($n = 2$; Fig. 5*B*) and in ACSF containing TTX and glutamate and GABA receptor antagonists ($n = 10$; Fig. 5*C*). All recorded neurons hyperpolarized by relaxin-3 were also sensitive to RXFP3-A2 (Fig. 5*D* and *E*), whereas only one of 10 recorded cells was insensitive to both peptides in the presence of glutamate and GABA receptor blockade.

### Relaxin peptide hormone does not influence the activity of a majority of PVN neurons

The influence of human H2 relaxin (H2; 600 nM), the cognate ligand for RXFP1, on spontaneous PVN neuron electrical activity was tested. Overall, 74% (14 of 19 cells) of recorded neurons remained unaffected by H2 application in normal ACSF. Of 19 PVN neurons, 12 were classified as type I putative magnocellular neurons and seven as type II putative parvocellular cells. Within a group of 12 type I neurons, mixed responses to bath application of H2 were observed; four neurons were depolarized by $1.7 \pm 0.9$ Hz (from $4.0 \pm 4.4$ to $6.7 \pm 5.2$ Hz) and one neuron was hyperpolarized by 3.5 mV. Notably, all type II neurons were unresponsive to H2 application (Fig. 6).

The biological activity of the H2 relaxin peptide used was verified by assessing its effects on the activity of subfornical organ neurons *in vitro*, as these cells are strongly excited by H2 relaxin (Sunn *et al.* 2002). In our test recordings, H2 relaxin (600 nM) increased the firing frequency of subfornical organ neurons by $2.6 \pm 1.4$ Hz ($n = 4$, data not shown).

### The majority of OT and AVP neurons express *RXFP3* mRNA

Oxytocin-positive neurons were numerous in the PaLM and PaV subdivisions of the PVN, while AVP-ir neurons were densely concentrated in the PaLM subdivision. The PaDC and PaMP subdivisions of the PVN displayed lower numbers of OT-ir and AVP-ir neurons (Table 1). Notably, the majority (91–100%) of AVP and OT neurons in all subdivisions of the PVN expressed *RXFP3* mRNA (Table 1 and Fig. 7).

### Relaxin-3-positive fibres are present in close vicinity to the lateral magnocellular PVN

Coronal sections through the PVN were immunostained for relaxin-3, OT and AVP ($n = 7$). An abundance of relaxin-3-containing fibres were detected within close vicinity of the PVN, along its entire rostrocaudal axis, but only rare relaxin-3-positive processes were detected within the PVN (Fig. 8). Single intra-PVN fibres were observed in apposition to both OT and AVP neurons (Fig. 8*C* and *D*).

### Nucleus incertus neurons innervate magnocellular PVN

A fluorescent RetroBeads tracer was injected unilaterally into the PVN of adult Wistar rats. Only brains in which the injection site was restricted to the magnocellular area of the PVN were used for quantitative cell counting analysis (Fig. 9). All tracing experiments were conducted using rats treated with colchicine ($n = 3$). Examination of the four brains areas in which relaxin-3 is synthesized in the rat (periaqueductal grey, raphe pontis, area dorsal to substantia nigra and the NI; Tanaka *et al.* 2005; Ma *et al.* 2007) revealed retrogradely labelled relaxin-3-positive neurons only in the NI. Individual ($38 \pm 13$) double-labelled neurons were scattered throughout all rostrocaudal NI levels (Fig. 9*C*). Single retrogradely filled, relaxin-3-negative neurons were also observed within the NI ($33 \pm 6$; Fig. 9*C* and *E*). Numerous RetroBeads-filled neurons were observed in the locus coeruleus, particularly ipsilateral to the injection site (Fig. 9*D*). In cases where the injection site extended beyond the boundary of the PVN (which were not included in the analysis), substantial numbers of backfilled relaxin-3-positive neurons were observed within the NI.

## Discussion

In the present study, we demonstrated a direct influence of native relaxin-3 and the truncated relaxin-3 analogue RXFP3-A2, which is a selective RXFP3 agonist, on electrical activity of type I magnocellular (OT- and AVP-synthesizing) neurons in rat PVN. We also detected a high level of colocalization of OT and AVP peptide immunoreactivity with *RXFP3* mRNA in the PVN, consistent with the involvement of RXFP3 in these effects. Conversely, we observed a lack of influence of RXFP3 activation on the electrical activity of a majority of type II parvocellular PVN neurons recorded. Moreover, we documented a lack of influence

of human relaxin peptide on the electrophysiological activity of a majority of putative magnocellular and all putative parvocellular PVN neurons tested. Immunohistochemical and neural tract-tracing studies demonstrated an abundant innervation of the peri-PVN area by relaxin-3-containing fibres and a sparse density of relaxin-3-positive fibres within the PVN, some of which originate from the pontine NI.

The PVN is a brain centre responsible for maintenance of homeostasis (sustaining physiological systems in a balance around optimal set-points) and, as such, it plays an essential role in the control of many autonomic functions, including food intake and energy expenditure

(Ferguson *et al.* 2008). Among many orexigenic factors (transmitters, peptides and hormones) acting within the hypothalamus, recent findings highlight the ability of the relaxin-3–RXFP3 signalling system to modulate food intake and identify the PVN as a potential target in this process (Ganella *et al.* 2013a). Importantly, after intra-PVN relaxin-3 injections in satiated rats, a primary behavioural change described was an increase in food consumption (McGowan *et al.* 2005). In contrast, other orexigenic peptides (such as orexin-A) may increase food intake as a consequence of increased spontaneous physical activity and arousal (for review, see Nixon *et al.* 2012). The strong orexigenic action of relaxin-3 after intra-PVN acute
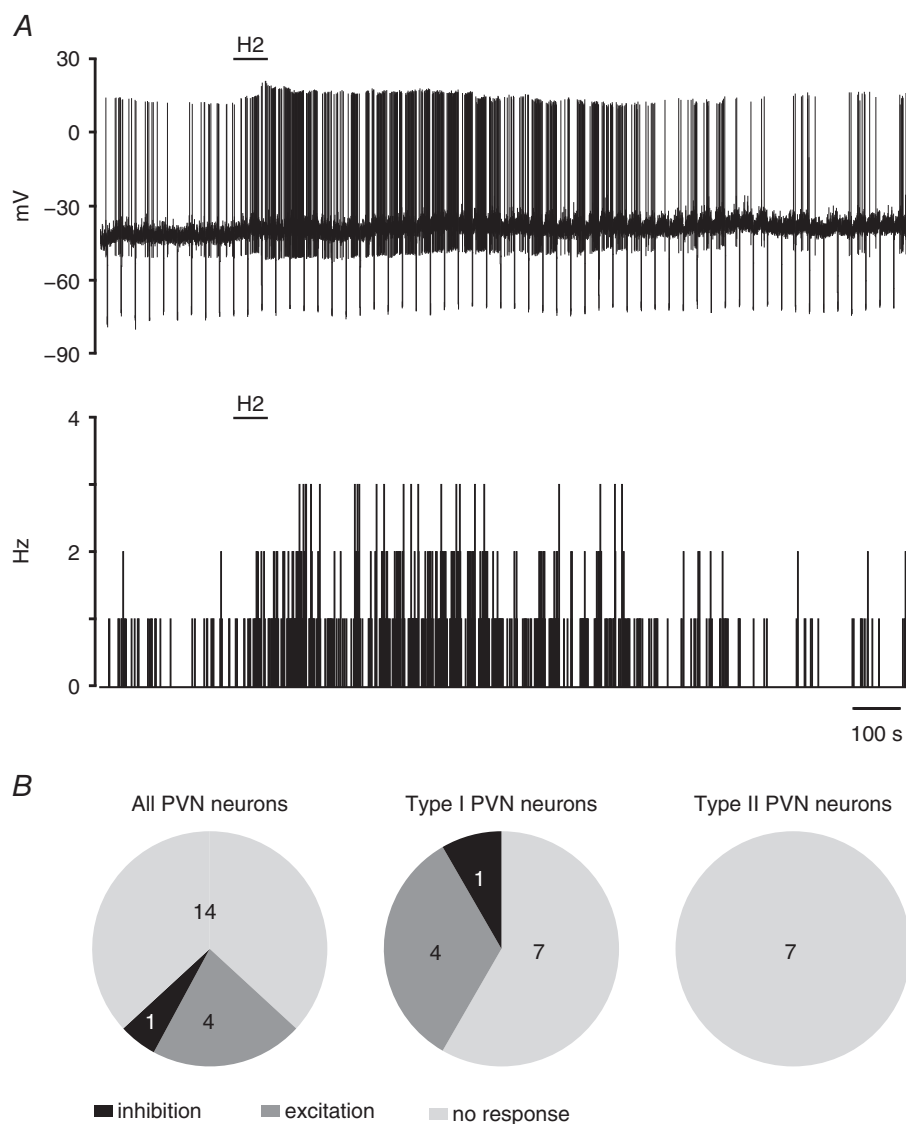


**Figure 6. Effect of H2 relaxin on type I and II PVN neurons**
*A*, representative trace of a zero current-clamp recording (upper) and corresponding activity histogram (lower; bin, 1 s) of a spontaneously active type I PVN neuron, illustrating the excitatory effect of H2 relaxin (H2; 600 nM; horizontal bar) in normal ACSF. *B*, pie charts representing the numbers of type I and II PVN neurons responding differentially to H2 relaxin application.

**Table 1. Number of neurons positive for AVP and OT immunoreactivity and percentage of AVP-ir and OT-ir neurons co-expressing *RXFP3* mRNA in the PVN**

| Peptide | PaLM | | PaDC | | PaMP | | PaV | |
|---|---|---|---|---|---|---|---|---|
| | Total cells | % RXFP3+ | Total cells | % RXFP3+ | Total cells | % RXFP3+ | Total cells | % RXFP3+ |
| AVP-ir | 73.6 ± 5.3 | 99.6 ± 0.2 | 4.8 ± 0.8 | 97.9 ± 2.1 | 17.4 ± 2.4 | 98.2 ± 1.0 | 15.2 ± 1.8 | 97.7 ± 1.1 |
| OT-ir | 44.0 ± 4.2 | 97.9 ± 0.8 | 17.5 ± 2.9 | 97.4 ± 1.1 | 19.9 ± 2.1 | 99.1 ± 0.6 | 48.9 ± 4.6 | 99.2 ± 0.4 |

The total number of neurons/cells represents the mean ± SEM of the neurons containing peptide immunoreactivity; and % RXFP3+ is the percentage of these neurons with AVP or OT immunoreactivity and *RXFP3* mRNA, as assessed in the outlined subnuclei in Fig. 7, in 30-$\mu$m-thick coronal brain sections collected between 1.72 and 1.80 mm caudal to bregma from six rats. Abbreviations: AVP, arginine vasopressin; ir, immunoreactivity; OT, oxytocin; PaDC, dorsal cap of the PVN; PaLM, lateral magnocellular part of the PVN; PaMP, medial parvocellular part of the PVN; PaV, ventral part of the PVN; and PVN, paraventricular nucleus.

and chronic injections (McGowan *et al.* 2005, 2006), along with an inhibitory influence of chronic hypothalamic RXFP3 activation on *OT* and *AVP* mRNA levels, strongly suggest that relaxin-3-induced changes in food intake involve an influence of RXFP3 activation on OT and AVP neuron activity. However, results from experiments that employ exogenous native relaxin-3 are potentially confounded by the fact that the peptide can activate the cognate receptor for the relaxin peptide hormone, RXFP1, which is also highly expressed in the rat PVN. Furthermore, RXFP1 activation leads to an increase in the intracellular concentration of cAMP, which can produce neuronal excitation (Burazin *et al.* 2005; Ma *et al.* 2006; Bathgate *et al.* 2013).

Electrophysiological data presented in the present study demonstrate a potent inhibitory influence of relaxin-3 and the selective RXFP3 agonist, RXFP3-A2, on the electrical activity of OT and AVP PVN neurons. In contrast to the high sensitivity of magnocellular PVN neurons to RXFP3 activation by native relaxin-3 and the selective agonist (88% and 82%, respectively), most type I cells studied were unresponsive to native human H2 relaxin peptide (52%). Moreover, all examined neurons were sensitive to both relaxin-3 and RXFP3-A2, which further suggests an involvement of RXFP3 in the action of relaxin-3. The blockade of G$\alpha_{i/o}$-proteins in tested PVN neurons prevented the inhibitory action of RXFP3-A2 in the majority of tested neurons, and these results are in accordance with previous studies conducted on RXFP3-expressing cell lines (Bathgate *et al.* 2013) and the first to demonstrate the involvement of G$\alpha_{i/o}$-proteins in intracellular signal transduction pathways activated by RXFP3 in PVN neurons. Finally, we demonstrated that both relaxin-3- and RXFP3-A2-evoked inhibition was blocked by the presence of the RXFP3 antagonist, R3 B1-22R. Interestingly, in the presence of RXFP3 antagonist, an increase in action potential firing was observed, which suggests a tonic inhibitory action of relaxin-3 on PVN neurons. Moreover, application of relaxin-3 in the presence of RXFP3 blockade caused an increase in action potential firing, which

might represent an unmasking of an excitatory action of relaxin-3 mediated by RXFP1. RXFP3 activation increases an outward whole-cell current that is sensitive to cadmium, a characteristic of calcium-dependent outward potassium currents described in magnocellular neurons (Cobbett *et al.* 1989; Li & Ferguson, 1996; Hlubek & Cobbett, 1997). In those studies, it was revealed that the whole-cell PVN neuron outward current is sensitive to tetraethylammonium. Therefore, an involvement of BK (big conductance) potassium channels in the described whole-cell current is possible (Barman *et al.* 2004). Importantly, BK channels were demonstrated to be involved in the inhibitory effect of other peptides, such as insulin and leptin (O'Malley *et al.* 2003; Yang *et al.* 2010). Likewise, the activity of BK channels is potentiated by activation of D2 dopamine and ET$_A$ endothelin receptors, and importantly, pertussis toxin treatment inhibits potentiation of whole-cell BK current (Twitchell & Rane, 1994; Kanyicska *et al.* 1997).

In addition to Ca$^{2+}$ and voltage, BK channel activity is regulated by protein kinases via protein phosphorylation (Lin *et al.* 2005). A downstream intracellular mechanism activated by RXFP3 is the phospholipase C/PKC pathway, and PKC can inhibit BK channels in different tissues, although activation of BK channels by PKC has also been reported (Barman *et al.* 2004; Zhu *et al.* 2006). Therefore, one of the possible signal transduction pathways involved in RXFP3 mediated inhibition of neuronal activity is PKC-dependent BK channel opening.

Another possible intracellular cascade activated by RXFP3 involves regulation of calcium influx in magnocellular PVN neurons. RXFP3 stimulation leads to reductions in cellular cAMP and/or activation of phosphatidylinositol 3-kinase-dependent or PKC-dependent mechanisms, and in a number of studies calcium influx was shown to be regulated by a stimulatory action of PKC on voltage-gated calcium channels (Stea *et al.* 1995; Love *et al.* 1998; Kamatchi *et al.* 2000; Scholze *et al.* 2001; Blumenstein *et al.* 2002). Therefore, calcium influx, a limiting factor for the outward current evoked by

the specific RXFP3 stimulation observed in our studies, may be a further effect of RXFP3-driven phospholipase C/PKC pathway activation.

The inhibitory action of relaxin-3 and RXFP3-A2 observed in the presence of voltage-sensitive $Na^+$ channel and glutamate/GABA receptor antagonists points to a postsynaptic location of RXFP3 on magnocellular OT and AVP PVN neurons. The postsynaptic localization of RXFP3 was further confirmed by *in situ* hybridization studies that revealed a high level of colocalization of *RXFP3* mRNA with OT and AVP peptide immunoreactivity in PVN neuronal cell bodies. Importantly, a postsynaptic localization of receptors for other neurotransmitters and hormones playing key roles in the control of metabolism and feeding behaviour, such as neuropeptide Y, $\alpha$-melanocyte-stimulating hormone and leptin, has been demonstrated on PVN neurons (Ghamari-Langroudi *et al.* 2011). However, it is important to consider that a confirmed postsynaptic localization of

RXFP3 on PVN neurons does not exclude a presynaptic occurrence of these receptors.

Despite the high density of *RXFP1* mRNA and [$^{33}$P]-relaxin binding sites present in rat PVN (Burazin *et al.* 2005; Ma *et al.* 2006) and the reported presence of putative relaxin-synthesizing neurons in magnocellular and parvocellular parts of the PVN (Sun *et al.* 2016), the breadth of influence of relaxin on spontaneous neuronal electrical activity within the nucleus is relatively minor (only 26% of all tested neurons were affected by H2 relaxin application in our brain slice preparation). However, activation of RXFP1 within the PVN may influence intracellular signalling cascades that do not affect the electrical activity of type II neurons (unlike in subfornical organ neurons) and cause transmitter release independently of electrical activity, as described for other peptides (e.g. AVP or OT; Sabatier *et al.* 2003; Ludwig *et al.* 2005).

In previous *in vivo* studies, the possible influence of the relaxin-3 system on the hypothalamic–pituitary
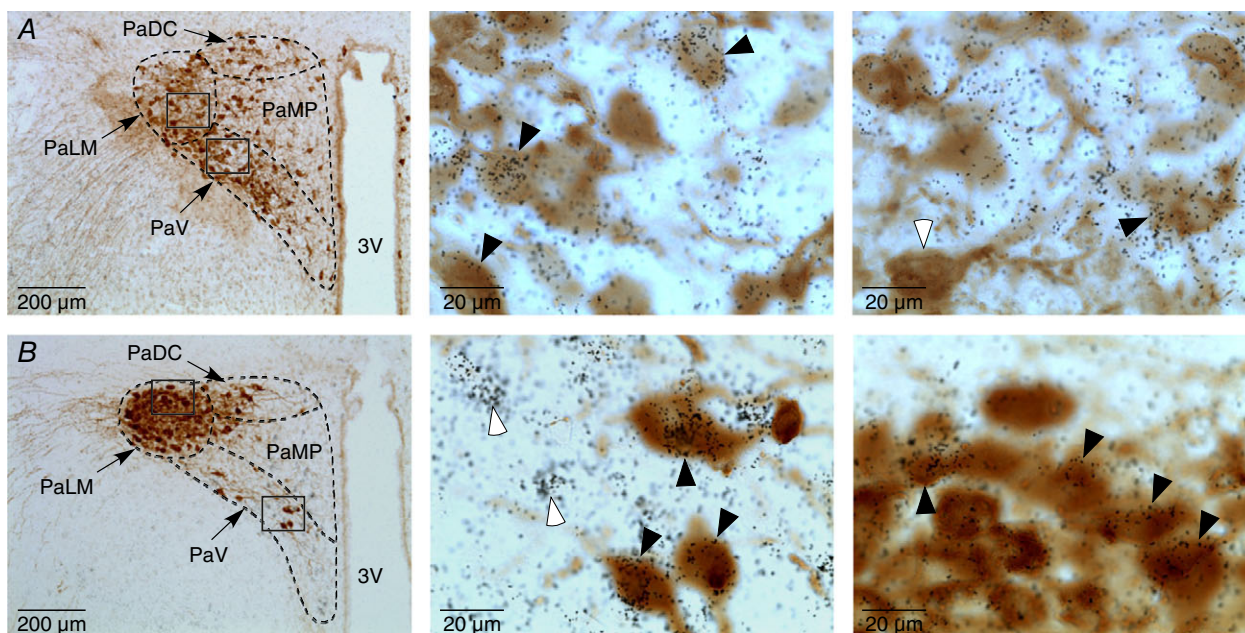


**Figure 7. Expression of *RXFP3* mRNA by OT and AVP PVN neurons**

*A*, left, low-power image of the paraventricular hypothalamic nucleus (PVN) of a rat, in which *RXFP3* mRNA was detected by *in situ* hybridization histochemistry and oxytocin (OT) was detected by immunohistochemistry; middle, high-magnification image of neurons in the ventral part of the PVN (PaV) outlined by a rectangle in the left panel; and right, high-magnification image of neurons in the lateral magnocellular part of the PVN (PaLM) outlined by a rectangle in the left panel. Some double-labelled neurons positive for OT-immunoreactivity (brown staining) and *RXFP3* mRNA (black silver grains) are indicated by black arrowheads. A white arrowhead in the right panel depicts an OT neuron negative for *RXFP3* mRNA. *B*, left, low-power image of the PVN of a rat, in which the expression of *RXFP3* mRNA was detected by *in situ* hybridization histochemistry and arginine vasopressin (AVP) was detected by immunohistochemistry; middle, high-magnification image of neurons in the ventral part of the PVN (PaV) outlined by a rectangle in the left panel; and right, high-magnification image of neurons in the lateral magnocellular part of the PVN (PaLM) outlined by a rectangle in the left panel. Some double-labelled neurons positive for AVP-immunoreactivity (brown staining) and *RXFP3* mRNA (black silver grains) are indicated by black arrowheads. Neurons expressing *RXFP3* mRNA but negative for AVP-immunoreactivity are indicated by white arrowheads. Abbreviations: 3V, third ventricle; PaDC, dorsal cap of PVN; PaLM, lateral magnocellular part of PVN; PaMP, medial parvocellular part of PVN; and PaV, ventral part of PVN. [Colour figure can be viewed at wileyonlinelibrary.com]
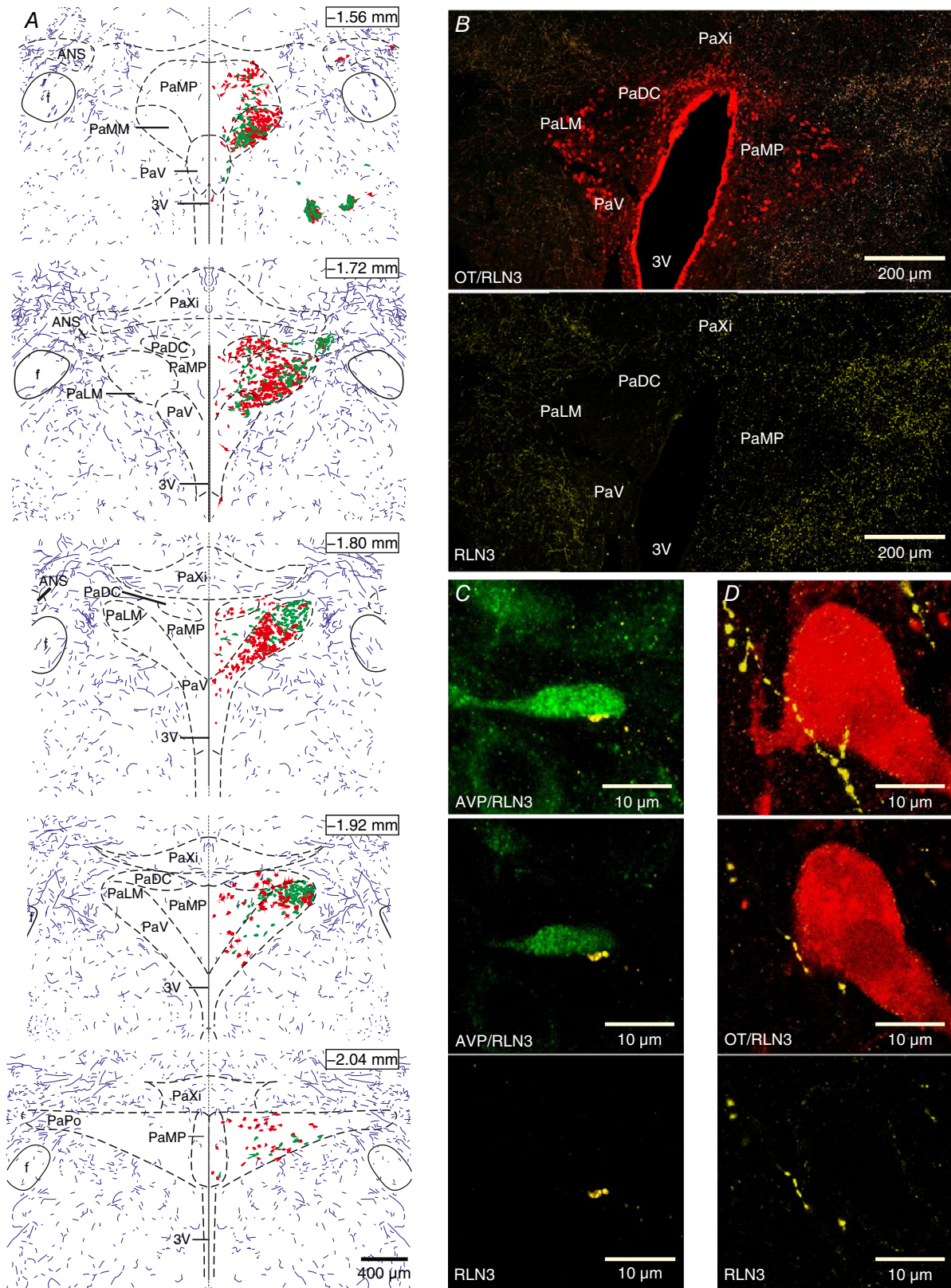
**Figure 8. Relaxin-3-positive fibres are present in close vicinity of the PVN**

*A*, reconstruction of the distribution of the relaxin-3-positive innervation (violet fibres) along with OT (red) and AVP (green) neurons, through the rostrocaudal axis of the PVN. Each section consists of a mirrored image through the

middle of the third ventricle (dashed line) of reconstructed relaxin-3 fibres with and without OT and AVP neurons, depicting the relative abundance of relaxin-3 fibres in the vicinity of the PVN compared with the nucleus boundary. The distance from bregma is indicated for each section. *B*, upper panel, confocal projection image of coronal rat brain section (40 $\mu$m thick) at the level of the PVN, illustrating relaxin-3 fibres (yellow) and OT-ir neurons (red); and lower panel, the same section with relaxin-3 fibres only. *C*, confocal projection image (upper) of sparse intra-PVN relaxin-3-ir fibre (yellow) in apposition with an AVP neuron (green); middle, single optical slice (1 $\mu$m) of merged image of AVP neuron and relaxin-3-ir fibre shown in upper image and single image of relaxin-3 fibre (lower). *D*, confocal projection image (upper) of intra-PVN relaxin-3-ir fibre (yellow) in apposition with an OT neuron (red); middle, single optical slice (1 $\mu$m) of merged image of OT neuron and relaxin-3-ir fibre shown in upper image and single image of relaxin-3 fibre (lower). Abbreviations: 3V, third ventricle; ANS, accessory neurosecretory nuclei; f, fornix; PaDC, dorsal cap of the PVN; PaLM, lateral magnocellular part of the PVN; PaMM, medial magnocellular part of the PVN; PaMP, medial parvocellular part of the PVN; PaPo, posterior part of the PVN; PaV ventral part of the PVN; and PaXi, paraxiphoid nucleus of thalamus. [Colour figure can be viewed at wileyonlinelibrary.com]

CRH–adrenocorticotrophic hormone (ACTH) system was investigated. Intra-PVN administration of 540 pmol relaxin-3 increased plasma ACTH and corticosterone concentrations in Wistar rats (McGowan *et al.* 2014). Independently, levels of c-*fos* and *CRH* mRNA were reported to be elevated in the PVN after the intra-cerebroventricular administration of relaxin-3 (Watanabe *et al.* 2011) in Sprague–Dawley rats, although there were no data provided relating to the direct or indirect nature of these effects. In our electrophysiological studies, in the majority of recorded type II PVN neurons we observed inhibitory responses to RXFP3 agonist (16 of 40 tested neurons) and rare excitatory responses (3 of 40 tested cells), but for technical reasons and for reasons relating to study design, we could not draw any conclusions about the possible CRH-positive nature of the tested neurons or the pre- *vs* postsynaptic site of the observed actions. Notably, the reported increase in plasma ACTH concentrations after intracerebroventricular and intra-PVN administration of relaxin-3 may depend on RXFP3-induced inhibition of OT release, as intra-PVN injections of an OT receptor antagonist enhanced basal secretion of ACTH into the blood (Neumann *et al.* 2000).

Among the putative parvocellular neurons sensitive to RXFP3 activation, we identified a population that were OT synthesizing. The role of parvocellular PVN OT signalling in control of metabolism is well established, and *OT* mRNA levels in both magno- and parvocellular neurons of the PVN are reduced by fasting (Kublaoui *et al.* 2008). Within the parvocellular OT neuron population are neurons that innervate the nucleus tractus solitarii (Rinaman, 1998), where OT modulates vagal efferent pathways and regulates gastric motility (McCann & Rogers, 1990). Thus, an inhibitory influence of RXFP3 signalling on OT parvocellular neuron activity may represent another element of the relaxin-3–RXFP3 control of metabolism.

Our previous studies have shown that long-lasting RXFP3 activation within the PVN and surrounds via virus-based secretion of a selective RXFP3 agonist, R3/I5, leads to a modest but consistent increase in food intake and body weight, and these changes are accompanied

by marked reductions in hypothalamic/PVN *OT* (50%) and *AVP* (25%) mRNA levels (Ganella *et al.* 2013*a*). The electrophysiological data collected in the present study have identified a cellular mechanism of RXFP3 activation within the PVN, revealing that OT and AVP neurons express *RXFP3* mRNA and functional receptors. Our observations that relaxin-3 and RXFP3-A2 activation of RXFP3 lead to inhibition of OT and AVP neurons are consistent with a dependence of the synthesis and release of these potent anorexigenic signals on neuronal activity (for review, see Ludwig & Leng, 2006; Sabatier *et al.* 2013; Pei *et al.* 2014) and indicate that these effects are likely to constitute a mechanism of relaxin-3-induced increase in food intake.

In our study, only sparse relaxin-3-containing fibres were revealed within the PVN by immunohistochemical staining in the presence of an extensive relaxin-3-ir innervation in the vicinity of the nucleus. In accordance with our immunohistochemical data revealing a sparse innervation of the PVN by relaxin-3-containing fibres, our neural tract-tracing studies identified only rare relaxin-3-synthesizing neurons throughout the brain innervating the PVN. All relaxin-3-positive neurons detected that innervated the PVN originated in the nucleus incertus. Comparable results were described by Ziegler *et al.* (2012), who identified a lack of retrogradely labelled neurons in the area of the NI after an injection of retrograde tracer, fluorogold, restricted to the magnocellular PVN. In the same study, in brains in which retrograde tracer diffused into the area neighbouring the PVN, a substantial number of backfilled neurons were detected in the NI, in line with our observations. Moreover, in brains with tracer correctly targeted to the PVN, RetroBeads-filled neurons were located unilaterally in the locus coeruleus, as seen in previous studies (Jones & Moore, 1977; Jones & Yang, 1985).

Our tract-tracing and immunohistochemical results are also in agreement with published anatomical data describing sparse processes originating from the NI in the area of PVN (Goto *et al.* 2001; Olucha-Bordonau *et al.* 2003) as well as a low number of relaxin-3 containing fibres within the PVN (Ma *et al.* 2007). The high sensitivity

of PVN neurons to both relaxin-3 and RXFP3-A2, along with the high density of *RXFP3* mRNA concurrent with a low density of relaxin-3 fibres within the nucleus is indicative of possible extrasynaptic actions of relaxin-3 within the PVN. The combination of a low-to-moderate abundance of relaxin-3-ir fibres and a high density of *RXFP3* mRNA was reported in the PVN and for some other brain structures in both rats and mice (for review, see Ganella *et al.* 2013*b*), strengthening the idea that in addition to conventional synaptic transmission that is associated with the relaxin-3–RXFP3 system (Ma *et al.*

2007; Blasiak *et al.* 2013, 2015), volume transmission by relaxin-3 may occur (for review, see Agnati *et al.* 2010). Moreover, interaction of relaxin-3-containing fibres with OT and AVP neuron dendrites, as described previously for inputs from limbic areas, is possible (Oldfield *et al.* 1985).

Furthermore, considering the close proximity of the PVN and periventricular and arcuate nuclei to the cerebral ventricular system and juxtaposition of the main group of neurons expressing relaxin-3 in the NI to the fourth ventricle, a neurohumoral pathway acting via the cerebrospinal fluid may also be involved
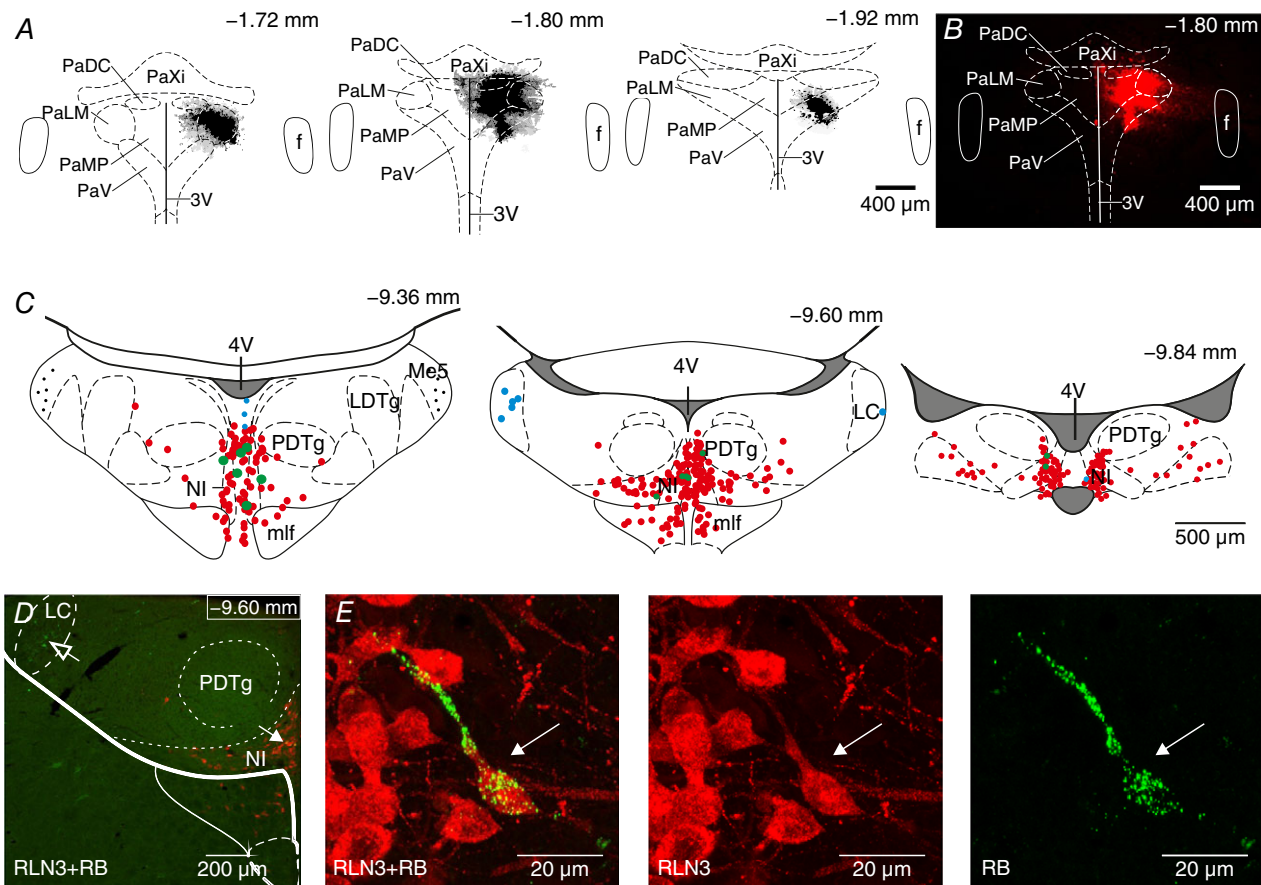


**Figure 9. Nucleus incertus relaxin-3 neurons innervate the PVN**
*A*, Schematic representation of consecutive coronal sections of paraventricular nucleus (PVN) and adjacent areas with the reconstruction of unilateral fluorescent RetroBeads retrograde tracer injection sites. The distance from bregma is indicated for each section. *B*, fluorescent microscopic image of a single coronal brain section. *C*, schematic reconstruction of the distribution of relaxin-3-ir neurons (red circles), relaxin-3-ir neurons filled with RetroBeads (RB; green circles) and relaxin-3-negative neurons filled with RB (blue circles) on selected rat coronal sections at the level of the NI (40 $\mu$m), following RB retrograde tracer injection into the PVN. The distance from bregma is indicated for each section. *D*, confocal microscopic image of a single coronal section at the level of the NI illustrating relaxin-3-ir neurons (red), relaxin-3/RB-ir neurons (green + red, solid arrow) and RB-positive/relaxin-3-negative neurons (green, open arrow). *E*, left panel, high-magnification projection image illustrating relaxin-3-ir neuron (red) containing granules of RetroBeads (green, indicated by arrow); middle panel, relaxin-3-ir-positive neurons; and right panel, the same neuron containing RB particles. Abbreviations: 3V, third ventricle; 4V, fourth ventricle; f, fornix; LDTg, laterodorsal tegmental nucleus; Me5, mesencephalic trigeminal nucleus; mlf, medial longitudinal fasciculus; NI, nucleus incertus; PaDC, dorsal cap of the PVN; PaLM, lateral magnocellular part of the PVN; PaMP, medial parvocellular part of the PVN; PaV ventral part of the PVN; PaXi, paraxiphoid nucleus of thalamus; and PDTg, posterodorsal tegmental nucleus. [Colour figure can be viewed at wileyonlinelibrary.com]

in relaxin-3 signalling, similar to that described for melanin-concentrating hormone signalling in the dorsal raphe nucleus (Torterolo *et al.* 2008).

The PVN is under the influence of a diverse range of neural inputs and neurotransmitters as well as humoral signals from the body, which enables adjustment of both internal processes and behaviour to the current needs of the organism. Regulation of food intake by RXFP3 modulation of PVN neuron activity represents a newly identified mode of homeostatic regulation of feeding, energy expenditure and hormonal balance in both physiological conditions and pathophysiological situations, and our data provide a likely cellular mechanism for RXFP3-dependent actions of relaxin-3. Importantly, strong activation of relaxin-3-containing neurons and relaxin-3 synthesis has been observed after central administration of CRH and in response to different neurogenic stressors (Tanaka *et al.* 2005; Banerjee *et al.* 2010), and a complex regulation of the relaxin-3–RXFP3 system was recently identified in rat models of stress-induced food intake (Lenglos *et al.* 2013; Calvez *et al.* 2016), which provides a particular impetus to research exploring the role of relaxin-3–RXFP3 signalling in stress-related eating disorders.

# References

Agnati LF, Guidolin D, Guescini M, Genedani S & Fuxe K (2010). Understanding wiring and volume transmission. *Brain Res Rev* **64**, 137–159.

Aoyagi T, Kusakawa S, Sanbe A, Hiroyama M, Fujiwara Y, Yamauchi J & Tanoue A (2009). Enhanced effect of neuropeptide Y on food intake caused by blockade of the $V_{1A}$ vasopressin receptor. *Eur J Pharmacol* **622**, 32–36.

Arletti R, Benelli A & Bertolini A (1990). Oxytocin inhibits food and fluid intake in rats. *Physiol Behav* **48**, 825–830.

Banerjee A, Shen PJ, Ma S, Bathgate RAD & Gundlach AL (2010). Swim stress excitation of nucleus incertus and rapid induction of relaxin-3 expression via CRF1 activation. *Neuropharmacology* **58**, 145–155.

Barman SA, Zhu S & White RE (2004). PKC activates BKCa channels in rat pulmonary arterial smooth muscle via cGMP-dependent protein kinase. *Am J Physiol Lung Cell Mol Physiol* **286**, L1275–1281.

Bathgate RAD, Halls ML, van der Westhuizen ET, Callander GE, Kocan M & Summers RJ (2013). Relaxin family peptides and their receptors. *Physiol Rev* **93**, 405–480.

Blasiak A, Blasiak T, Lewandowski MH, Hossain MA, Wade JD & Gundlach AL (2013). Relaxin-3 innervation of the intergeniculate leaflet of the rat thalamus – neuronal tract-tracing and *in vitro* electrophysiological studies. *Eur J Neurosci* **37**, 1284–1294.

Blasiak A, Siwiec M, Grabowiecka A, Blasiak T, Czerw A, Blasiak E, Kania A, Rajfur Z, Lewandowski MH & Gundlach AL (2015). Excitatory orexinergic innervation of rat *nucleus incertus* – implications for ascending arousal, motivation and feeding control. *Neuropharmacology* **99**, 432–447.

Blumenstein Y, Kanevsky N, Sahar G, Barzilai R, Ivanina T & Dascal N (2002). A novel long N-terminal isoform of human L-type $Ca^{2+}$ channel is up-regulated by protein kinase C. *J Biol Chem* **277**, 3419–3423.

Boudaba C, Di S & Tasker JG (2003). Presynaptic noradrenergic regulation of glutamate inputs to hypothalamic magnocellular neurones. *J Neuroendocrinol* **15**, 803–810.

Bourque CW (1986). Calcium-dependent spike after-current induces burst firing in magnocellular neurosecretory cells. *Neurosci Lett* **70**, 204–209.

Burazin TCD, Bathgate RAD, Macris M, Layfield S, Gundlach AL & Tregear GW (2002). Restricted, but abundant, expression of the novel rat gene-3 (R3) relaxin in the dorsal tegmental region of brain. *J Neurochem* **82**, 1553–1557.

Burazin TCD, Johnson KJ, Ma S, Bathgate RAD, Tregear GW & Gundlach AL (2005). Localization of LGR7 (relaxin receptor) mRNA and protein in rat forebrain: correlation with relaxin binding site distribution. *Ann NY Acad Sci* **1041**, 205–210.

Calvez J, de Avila C, Matte LO, Guèvremont G, Gundlach AL & Timofeeva E (2016). Role of relaxin-3/RXFP3 system in stress-induced binge-like eating in female rats. *Neuropharmacology* **102**, 207–215.

Calvez J, Lenglos C, de Avila C, Guèvremont G & Timofeeva E (2015). Differential effects of central administration of relaxin-3 on food intake and hypothalamic neuropeptides in male and female rats. *Genes Brain Behav* **14**, 550–563.

Cobbett P, Legendre P & Mason WT (1989). Characterization of three types of potassium current in cultured neurones of rat supraoptic nucleus area. *J Physiol* **410**, 443–462.

Drummond GB (2009). Reporting ethical matters in *The Journal of Physiology*: standards and advice. *J Physiol* **587**, 713–719.

Ferguson AV, Latchford KJ & Samson WK (2008). The paraventricular nucleus of the hypothalamus – a potential target for integrative treatment of autonomic dysfunction. *Expert Opin Ther Targets* **12**, 717–727.

Ganella DE, Callander GE, Ma S, Bye CR, Gundlach AL & Bathgate RAD (2013*a*). Modulation of feeding by chronic rAAV expression of a relaxin-3 peptide agonist in rat hypothalamus. *Gene Ther* **20**, 703–716.

Ganella DE, Ma S & Gundlach AL (2013*b*). Relaxin-3/RXFP3 signalling and neuroendocrine function – a perspective on extrinsic hypothalamic control. *Front Endocrinol (Lausanne)* **4**, 128.

Ghamari-Langroudi M, Srisai D & Cone RD (2011). Multinodal regulation of the arcuate/paraventricular nucleus circuit by leptin. *Proc Natl Acad Sci USA* **108**, 355–360.

Goto M, Swanson LW & Canteras NS (2001). Connections of the nucleus incertus. *J Comp Neurol* **438**, 86–122.

Halls ML, Bathgate RAD, Sutton SW, Dschietzig TB & Summers RJ (2015). International Union of Basic and Clinical Pharmacology. XCV. Recent advances in the understanding of the pharmacology and biological roles of relaxin family peptide receptors 1–4, the receptors for relaxin family peptides. *Pharmacol Rev* **67**, 389–440.

Haugaard-Kedström LM, Shabanpoor F, Hossain MA, Clark RJ, Ryan PJ, Craik DJ, Gundlach AL, Wade JD, Bathgate RAD & Rosengren KJ (2011). Design, synthesis, and characterization of a single-chain peptide antagonist for the relaxin-3 receptor RXFP3. *J Am Chem Soc* **133**, 4965–4974.

Hazell GG, Hindmarch CC, Pope GR, Roper JA, Lightman SL, Murphy D, O'Carroll AM & Lolait SJ (2012). G protein-coupled receptors in the hypothalamic paraventricular and supraoptic nuclei – serpentine gateways to neuroendocrine homeostasis. *Front Neuroendocrinol* **33**, 45–66.

Hida T, Takahashi E, Shikata K, Hirohashi T, Sawai T, Seiki T, Tanaka H, Kawai T, Ito O, Arai T, Yokoi A, Hirakawa T, Ogura H, Nagasu T, Miyamoto N & Kuromitsu J (2006). Chronic intracerebroventricular administration of relaxin-3 increases body weight in rats. *J Recept Signal Transduct Res* **26**, 147–158.

Hille B (2001). *Ion Channels of Excitable Membranes*. Sinauer, Sunderland, MA, USA.

Hlubek MD & Cobbett P (1997). Outward potassium currents of supraoptic magnocellular neurosecretory cells isolated from the adult guinea-pig. *J Physiol* **502**, 61–74.

Jones BE & Moore RY (1977). Ascending projections of the locus coeruleus in the rat. II. Autoradiographic study. *Brain Res* **127**, 25–53.

Jones BE & Yang TZ (1985). The efferent projections from the reticular formation and the locus coeruleus studied by anterograde and retrograde axonal transport in the rat. *J Comp Neurol* **242**, 56–92.

Kamatchi GL, Tiwari SN, Durieux ME & Lynch C, 3rd (2000). Effects of volatile anesthetics on the direct and indirect protein kinase C-mediated enhancement of alpha1E-type Ca(2+) current in Xenopus oocytes. *J Pharmacol Exp Ther* **293**, 360–369.

Kanyicska B, Freeman ME & Dryer SE (1997). Endothelin activates large-conductance $K^+$ channels in rat lactotrophs: reversal by long-term exposure to dopamine agonist. *Endocrinology* **138**, 141–3153.

Kim YR, Eom JS, Yang JW, Kang J & Treasure J (2015). The impact of oxytocin on food intake and emotion recognition in patients with eating disorders: a double blind single dose within-subject cross-over design. *PLoS One* **10**, e0137514.

Klockars A, Levine AS & Olszewski PK (2015). Central oxytocin and food intake: focus on macronutrient-driven reward. *Front Endocrinol (Lausanne)* **6**, 65.

Kublaoui BM, Gemelli T, Tolson KP, Wang Y & Zinn AR (2008). Oxytocin deficiency mediates hyperphagic obesity of *Sim1* haploinsufficient mice. *Mol Endocrinol* **22**, 1723–1734.

Kuei C, Sutton S, Bonaventure P, Pudiak C, Shelton J, Zhu J, Nepomuceno D, Wu J, Chen J, Kamme F, Seierstad M, Hack MD, Bathgate RAD, Hossain MA, Wade JD, Atack J, Lovenberg TW & Liu C (2007). R3(BΔ23-27)R/I5 chimeric peptide, a selective antagonist for GPCR135 and GPCR142 over relaxin receptor LGR7: in vitro and in vivo characterization. *J Biol Chem* **282**, 25425–25435.

Lee SK, Lee S, Shin SY, Ryu PD & Lee SY (2012). Single cell analysis of voltage-gated potassium channels that determines neuronal types of rat hypothalamic paraventricular nucleus neurons. *Neuroscience* **205**, 49–62.

Lenglos C, Calvez J & Timofeeva E (2015). Sex-specific effects of relaxin-3 on food intake and brain expression of corticotropin-releasing factor in rats. *Endocrinology* **156**, 523–533.

Lenglos C, Mitra A, Guèvremont G & Timofeeva E (2013). Sex differences in the effects of chronic stress and food restriction on body weight gain and brain expression of CRF and relaxin-3 in rats. *Genes Brain Behav* **12**, 370–387.

Lenglos C, Mitra A, Guèvremont G & Timofeeva E (2014). Regulation of expression of relaxin-3 and its receptor RXFP3 in the brain of diet-induced obese rats. *Neuropeptides* **48**, 119–132.

Li Z & Ferguson AV (1996). Electrophysiological properties of paraventricular magnocellular neurons in rat brain slices: modulation of IA by angiotensin II. *Neuroscience* **71**, 133–145.

Lin MT, Longo LD, Pearce WJ & Hessinger DA (2005). $Ca^{2+}$-activated $K^+$ channel-associated phosphatase and kinase activities during development. *Am J Physiol Heart Circ Physiol* **289**, H414–425.

Liu C, Eriste E, Sutton S, Chen J, Roland B, Kuei C, Farmer N, Jornvall H, Sillard R & Lovenberg TW (2003). Identification of relaxin-3/INSL7 as an endogenous ligand for the orphan G-protein-coupled receptor GPCR135. *J Biol Chem* **278**, 50754–50764.

Love JA, Richards NW, Owyang C & Dawson DC (1998). Muscarinic modulation of voltage-dependent $Ca^{2+}$ channels in insulin-secreting HIT-T15 cells. *Am J Physiol* **274**, G397–405.

Ludwig M, Bull PM, Tobin VA, Sabatier N, Landgraf R, Dayanithi G & Leng G (2005). Regulation of activity-dependent dendritic vasopressin release from rat supraoptic neurones. *J Physiol* **564**, 515–522.

Ludwig M & Leng G (2006). Dendritic peptide release and peptide-dependent behaviours. *Nat Rev Neurosci* **7**, 126–136.

Luther JA & Tasker JG (2000). Voltage-gated currents distinguish parvocellular from magnocellular neurones in the rat hypothalamic paraventricular nucleus. *J Physiol* **523**, 193–209.

Ma S, Blasiak A, Olucha-Bordonau FE, Verberne AJ & Gundlach AL (2013). Heterogeneous responses of nucleus incertus neurons to corticotrophin-releasing factor and coherent activity with hippocampal theta rhythm in the rat. *J Physiol* **591**, 3981–4001.

Ma S, Bonaventure P, Ferraro T, Shen PJ, Burazin TCD, Bathgate RAD, Liu C, Tregear GW, Sutton SW & Gundlach AL (2007). Relaxin-3 in GABA projection neurons of nucleus incertus suggests widespread influence on forebrain circuits via G-protein-coupled receptor-135 in the rat. *Neuroscience* **144**, 165–190.

Ma S, Roozendaal B, Burazin TCD, Tregear GW, McGaugh JL & Gundlach AL (2005). Relaxin receptor activation in the basolateral amygdala impairs memory consolidation. *Eur J Neurosci* **22**, 2117–2122.

Ma S, Shen PJ, Burazin TCD, Tregear GW & Gundlach AL (2006). Comparative localization of leucine-rich repeat-containing G-protein-coupled receptor-7 (RXFP1) mRNA and [$^{33}$P]-relaxin binding sites in rat brain: restricted somatic co-expression a clue to relaxin action? *Neuroscience* **141**, 329–344.

McCann MJ & Rogers RC (1990). Oxytocin excites gastric-related neurones in rat dorsal vagal complex. *J Physiol* **428**, 95–108.

McGowan BM, Minnion JS, Murphy KG, Roy D, Stanley SA, Dhillo WS, Gardiner JV, Ghatei MA & Bloom SR (2014). Relaxin-3 stimulates the neuro-endocrine stress axis via corticotrophin-releasing hormone. *J Endocrinol* **221**, 337–346.

McGowan BM, Stanley SA, Smith KL, Minnion JS, Donovan J, Thompson EL, Patterson M, Connolly MM, Abbott CR, Small CJ, Gardiner JV, Ghatei MA & Bloom SR (2006). Effects of acute and chronic relaxin-3 on food intake and energy expenditure in rats. *Regul Pept* **136**, 72–77.

McGowan BM, Stanley SA, Smith KL, White NE, Connolly MM, Thompson EL, Gardiner JV, Murphy KG, Ghatei MA & Bloom SR (2005). Central relaxin-3 administration causes hyperphagia in male Wistar rats. *Endocrinology* **146**, 3295–3300.

Meyer AH, Langhans W & Scharrer E (1989). Vasopressin reduces food intake in goats. *Q J Exp Physiol* **74**, 465–473.

Morton GJ, Thatcher BS, Reidelberger RD, Ogimoto K, Wolden-Hanson T, Baskin DG, Schwartz MW & Blevins JE (2012). Peripheral oxytocin suppresses food intake and causes weight loss in diet-induced obese rats. *Am J Physiol Endocrinol Metab* **302**, E134–E144.

Neumann ID, Krömer SA, Toschi N & Ebner K (2000). Brain oxytocin inhibits the (re)activity of the hypothalamo–pituitary–adrenal axis in male rats: involvement of hypothalamic and limbic brain regions. *Regul Pept* **96**, 31–38.

Nixon JP, Kotz CM, Novak CM, Billington CJ & Teske JA (2012). Neuropeptides controlling energy balance: orexins and neuromedins. *Handb Exp Pharmacol* **209**, 77–109.

Oldfield BJ, Hou-Yu A & Silverman AJ (1985). A combined electron microscopic HRP and immunocytochemical study of the limbic projections to rat hypothalamic nuclei containing vasopressin and oxytocin neurons. *J Comp Neurol* **231**, 221–231.

Olucha-Bordonau FE, Teruel V, Barcia-González J, Ruiz-Torner A, Valverde-Navarro AA & Martínez-Soriano F (2003). Cytoarchitecture and efferent projections of the nucleus incertus of the rat. *J Comp Neurol* **464**, 62–97.

O'Malley D, Shanley LJ & Harvey J (2003). Insulin inhibits rat hippocampal neurones via activation of ATP-sensitive K$^+$ and large conductance Ca$^{2+}$-activated K$^+$ channels. *Neuropharmacology* **44**, 855–863.

Paxinos G & Watson C (2007). *The Rat Brain in Stereotaxic Coordinates*. Elsevier, San Diego, CA, USA.

Pei H, Sutton AK, Burnett KH, Fuller PM & Olson DP (2014). AVP neurons in the paraventricular nucleus of the hypothalamus regulate feeding. *Mol Metab* **3**, 209–215.

Rinaman L (1998). Oxytocinergic inputs to the nucleus of the solitary tract and dorsal motor nucleus of the vagus in neonatal rats. *J Comp Neurol* **399**, 101–109.

Sabatier N, Caquineau C, Dayanithi G, Bull P, Douglas AJ, Guan XM, Jiang M, Van der Ploeg L & Leng G (2003). α-Melanocyte-stimulating hormone stimulates oxytocin release from the dendrites of hypothalamic neurons while inhibiting oxytocin release from their terminals in the neurohypophysis. *J Neurosci* **23**, 10351–10358.

Sabatier N, Leng G & Menzies J (2013). Oxytocin, feeding, and satiety. *Front Endocrinol (Lausanne)* **4**, 35.

Scholze A, Plant TD, Dolphin AC & Nurnberg B (2001). Functional expression and characterization of a voltage-gated CaV1.3 (alpha1D) calcium channel subunit from an insulin-secreting cell line. *Mol Endocrinol* **15**, 1211–1221.

Shabanpoor F, Akhter Hossain M, Ryan PJ, Belgi A, Layfield S, Kocan M, Zhang S, Samuel CS, Gundlach AL, Bathgate RAD, Separovic F & Wade JD (2012). Minimization of human relaxin-3 leading to high-affinity analogues with increased selectivity for relaxin-family peptide 3 receptor (RXFP3) over RXFP1. *J Med Chem* **55**, 1671–1681.

Sherwood OD (2004). Relaxin's physiological roles and other diverse actions. *Endocr Rev* **25**, 205–234.

Smith CM, Ryan PJ, Hosken IT, Ma S & Gundlach AL (2011). Relaxin-3 systems in the brain—the first 10 years. *J Chem Neuroanat* **42**, 262–275.

Smith CM, Shen PJ, Banerjee A, Bonaventure P, Ma S, Bathgate RAD, Sutton SW & Gundlach AL (2010). Distribution of relaxin-3 and RXFP3 within arousal, stress, affective, and cognitive circuits of mouse brain. *J Comp Neurol* **518**, 4016–4045.

Stea A, Soong TW & Snutch TP (1995). Determinants of PKC-dependent modulation of a family of neuronal calcium channels. *Neuron* **15**, 929–940.

Sun HJ, Chen D, Han Y, Zhou YB, Wang JJ, Chen Q, Li YH, Gao XY, Kang YM & Zhu GQ (2016). Relaxin in paraventricular nucleus contributes to sympathetic overdrive and hypertension via PI3K-Akt pathway. *Neuropharmacology* **103**, 247–256.

Sunn N, Egli M, Burazin TC, Burns P, Colvill L, Davern P, Denton DA, Oldfield BJ, Weisinger RS, Rauch M, Schmid HA & McKinley MJ (2002). Circulating relaxin acts on subfornical organ neurons to stimulate water drinking in the rat. *Proc Natl Acad Sci USA* **99**, 1701–1706.

Tanaka M, Iijima N, Miyamoto Y, Fukusumi S, Itoh Y, Ozawa H & Ibata Y (2005). Neurons expressing relaxin 3/INSL 7 in the nucleus incertus respond to stress. *Eur J Neurosci* **21**, 1659–1670.

Timofeeva E, Baraboi ED & Richard D (2005). Contribution of the vagus nerve and lamina terminalis to brain activation induced by refeeding. *Eur J Neurosci* **22**, 1489–1501.

Torterolo P, Lagos P, Sampogna S & Chase MH (2008). Melanin-concentrating hormone (MCH) immunoreactivity in non-neuronal cells within the raphe nuclei and subventricular region of the brainstem of the cat. *Brain Res* **1210**, 163–178.

Twitchell WA & Rane SG (1994). Nucleotide-independent modulation of Ca(2+)-dependent K$^+$ channel current by a mu-type opioid receptor. *Mol pharmacol* **46**, 793–798.

van der Westhuizen ET, Werry TD, Sexton PM & Summers RJ (2007). The relaxin family peptide receptor 3 activates extracellular signal-regulated kinase 1/2 through a protein kinase C-dependent mechanism. *Mol Pharmacol* **71**, 1618–1629.

Watanabe Y, Miyamoto Y, Matsuda T & Tanaka M (2011). Relaxin-3/INSL7 regulates the stress-response system in the rat hypothalamus. *J Mol Neurosci* **43**, 169–174.

Weisinger RS, Burns P, Eddie LW & Wintour EM (1993). Relaxin alters the plasma osmolality-arginine vasopressin relationship in the rat. *J Endocrinol* **137**, 505–510.

Yang MJ, Wang F, Wang JH, Wu WN, Hu ZL, Cheng J, Yu DF, Long LH, Fu H, Xie N & Chen JG (2010). PI3K integrates the effects of insulin and leptin on large-conductance $Ca^{2+}$-activated $K^+$ channels in neuropeptide Y neurons of the hypothalamic arcuate nucleus. *Am J Physiol Endocrinol Metab* **298**, E193–201.

Zhu S, White RE & Barman SA (2006). Effect of PKC isozyme inhibition on forskolin-induced activation of BKCa channels in rat pulmonary arterial smooth muscle. *Lung* **184**, 89–97.

Ziegler DR, Edwards MR, Ulrich-Lai YM, Herman JP & Cullinan WE (2012). Brainstem origins of glutamatergic innervation of the rat hypothalamic paraventricular nucleus. *J Comp Neurol* **520**, 2369–2394.

## Additional information

### Competing interests

None declared.

### Author contributions

A.B. and A.L.G. conceived the project. A.B., A.K., A.G., T.B., A.G., Z.R., M.H.L., G.H., C.d.A., E.T. and A.L.G. contributed to the design of the experiments. A.K. performed, analysed and interpreted the *in vitro* electrophysiology data. A.G. and A.G. performed the neural tract tracing and immunohistochemical staining and analysed and interpreted the resultant microscopy data. T.B. performed the neural tract-tracing experiments. C.d.A. and E.T. performed and interpreted *in situ* hybridization experiments. A.B. designed, performed and interpreted the *in vitro* electrophysiology and immunohistochemistry experiments and wrote the article. A.B. and A.L.G. revised the article, and all authors provided comments and corrections. All authors approved the final version of the manuscript and agree to be accountable for all aspects of the work in ensuring that questions related to the accuracy or integrity of any part of the work are appropriately investigated and resolved. All persons designated as authors qualify for authorship, and all those who qualify for authorship are listed.